Research Article

Mediterranean Marine Science
Indexed in WoS (Web of Science, ISI Thomson) and SCOPUS
www.hcmr.gr
DOI: https://doi.org/10.12681/mms.40914

Contribution to the Special Issue: Marine Animal Forest of the World (MAF WORLD)

Mapping and Conservation of Cold-Water Corals in the Lacaze-Duthiers Canyon for Transboundary Management

Marie-Claire FABRI[1], Jeanne DREIDEMY[1], Claude ESTOURNEL[2], Sandrine VAZ[3], Noëmie MICHEZ[4], Pere PUIG[5] , and Franck LARTAUD[6]

[1] Ifremer Centre de Méditerranée, Département Océanographie et Dynamique des Ecosystèmes, COAST, 83500 La Seyne sur Mer, France
[2] Laboratoire d'Etudes en Géophysique et Océanographie Spatiales (LEGOS), CNRS/UPS/CNES/IRD, Avenue Edouard Belin 14, 31400 Toulouse, France
[3] MARBEC, Univ Montpellier, CNRS, Ifremer, IRD, Sète, France
[4] Parc naturel marin du golfe du Lion, Office français de la Biodiversité, 2 impasse de Charlemagne, 66700 Argelès-sur-mer, France
[5] Institut de Ciències del Mar, ICM-CSIC, Barcelona, Spain
[6] Sorbonne Université, CNRS, Laboratoire d'Ecogéochimie des Environnements Benthiques (LECOB), Observatoire Océanologique de Banyuls, 66650 Banyuls-sur-Mer, France

Corresponding author: Marie-Claire Fabri; Marie.Claire.Fabri@ifremer.fr

Contributing Editor: Sergio ROSSI

Received: 25 March 2025; Accepted: 27 May 2025; Published online: 05 June 2025

Abstract

Cold-water coral habitats (*Madrepora oculata* and *Desmophyllum pertusum*) were mapped in the Lacaze-Duthiers Canyon, within the "Parc naturel marin du golfe du Lion" (northwestern Mediterranean), to support the creation of a strongly protected area for these vulnerable marine ecosystems (VME). The analyses are based on ROV data, high-resolution digital terrain models (5–10 m), hydrodynamic model simulations (currents, temperature, salinity from SYMPHONIE), and fishing pressure data derived from Vessel Monitoring System (VMS) and Automatic Identification System (AIS) fishing data. Habitat models indicate coral habitats are mainly on the western canyon flank (250 to 600 m depth). *Desmophyllum pertusum* predominantly colonizes gentle slopes at cliff bases, while *M. oculata* is found on steeper slopes, and the eastern flank. Some western flank areas support both species. Direct impacts from fishing activities, including lost longlines and nets entangled with corals, were observed. In addition, bottom trawling at the continental shelf edge induces sediment resuspension, potentially smothering the underlying coral ecosystems in the canyon. This study recommends enhancing fishing activity monitoring by increasing VMS positioning transmission frequency across European countries and facilitating the combination of VMS and AIS data to derive higher-resolution fishing effort and footprint assessments. Protection should prioritize canyon flanks and the surrounding continental shelf, not just the canyon itself, to mitigate fishing pressure. Tailored management measures are needed for sensitive habitats. Creating a strongly protected area will require crossborder cooperation (France, Spain) to ensure the effective conservation of these fragile ecosystems.

Keywords: Animal forests; Marine protected areas (MPA); Fishing impact; Derelict fishing gears; Conservation strategies; Northwestern Mediterranean.

Introduction

Submarine canyons with hard substrates frequently host sessile species known as "engineering" or "structuring" organisms. These species create habitats that provide shelter, feeding, and breeding grounds for other organisms, forming what are referred to as animal forests (Bramanti *et al.*, 2017). These reef habitats are now protected under various conventions at international (FAO, 2016), European (EU, 1992, 2008a), and Mediterranean levels (GFCM, 2009, 2018, 2019).

Deep-sea trawling, particularly on the continental shelf break and upper slope, is a significant threat to deep-sea ecosystems globally (Eigaard *et al.*, 2017; Amoroso *et al.*, 2018). Chronically trawled sediments exhibit substantial reductions in organic matter content (up to 52%) and a slowdown in organic carbon turnover (~ 37%) (Pusceddu *et al.*, 2014). Submarine canyons incising the world's continental shelves and slopes play a crucial role in safeguarding benthic species from bottom

trawling (Puig & Gili, 2019). The steep slopes of these canyons, eroded by currents and sediment failures, often expose outcropping rocks that act as natural barriers to trawl gears. However, canyon ecosystems can still be affected by the indirect impacts of sediments resuspended by trawling on the overlying continental slopes and shelves (Durrieu de Madron *et al.*, 2005; Martin *et al.*, 2008; Puig *et al.*, 2012). This sediment influx settling in the canyons does not serve as a food source, but rather buries and suffocates the benthic species residing there (Bilan *et al.*, 2023).

Other fishing gear types, such as longlines and gillnets, also impact ecosystem engineer species like scleractinians, antipatharians, and large octocorals living within submarine canyons. While these gears do not physically destroy the seabed like trawl gear, they can cause significant harm when they become entangled with the rigid skeletons of arborescent species. This leads to colony breakage as fishermen attempt to retrieve their gear, causing further disruption to the ecosystem (Ragnarsson *et al.*, 2017).

To protect deep-sea species from both direct and indirect fishing impacts, the establishment of Marine Protected Areas (MPAs) and, within these, Strong Protection Zones, is essential. On July 12, 2023, the European Parliament adopted the "Nature Restoration Act," which mandates Member States to implement restoration measures for at least 20% of all EU terrestrial and marine protected areas by 2030, and for all ecosystems in need of restoration by 2050 (EU, 2023). Ecosystem restoration can be either passive, which involves halting anthropogenic pressure and allowing natural regeneration, or active, which requires human intervention to assist species recovery. A passive restoration measure, such as the creation of a Strong Protection Zone, involves completely stopping human activities in vulnerable marine ecosystems (VMEs). A Strong Protection Zone must meet three criteria: 1) the cessation of anthropogenic pressures; 2) regulatory protection, such as being part of a marine protected area; and 3) the effective enforcement of regulations. Identifying ecologically sensitive areas with remarkable marine biodiversity is the first step in establishing a Strong Protection Zone to enhance the protection of specific species or habitats.

The "Parc naturel marin du golfe du Lion", located in the northwestern Mediterranean, encompasses several canyons, including the Lacaze-Duthiers Canyon. This canyon is known for hosting large colonies of structuring scleractinian benthic species on both canyon flanks that conform with the criteria that determine a VME. The presence of scleractinian species in the Lacaze-Duthiers Canyon, was documented early on in the literature (Lacaze-Duthiers, 1897; Peres & Picard, 1964) and characterized through J-Y Cousteau's pioneering 'Diving saucer' dives (Reyss, 1964). Since then, numerous scientific studies have enhanced our understanding of this canyon, which is one of eleven canyons studied extensively, with over 50 publications (Matos *et al.*, 2018). However, the distribution of these animal forest species across the canyon has not yet been fully mapped, despite existing distribution data derived from ROV surveys (Fiala-Medioni *et al.*, 2012; Watremez, 2012; Gori *et al.*, 2013; Fabri *et al.*, 2014; Lartaud *et al.*, 2017; Fabri *et al.*, 2022). More specifically, the scleractinian species present in this canyon create biogenic habitats supporting a diverse array of associated species which are attractive to predators. Despite their richness and diversity, these areas are subject to ongoing anthropogenic pressures.

All the ROV coral observations we have in the canyon are considered point data, as opposed to surface data, because the ROV only captures what is illuminated within the beam of its searchlights. Exploring the entire canyon region exhaustively with an ROV is unrealistic, as it would be too time-consuming and expensive, much like trying to explore a canyon in the dark with a flashlight. Consequently, predictive habitat modeling is a very useful technique for estimating the distribution of a habitat when terrain or environmental characteristics are known. It uses statistical methods to identify relationships between known species occurrences and environmental variables, and then projects these relationships across unsampled areas (Elith *et al.*, 2011; Phillips *et al.*, 2019). Predictive habitat modeling allows examining the relationships among terrain and environmental variables and the presence or absence of species, thereby forecasting suitable habitats for species establishment (Davies *et al.*, 2008; Davies & Guinotte, 2011). This approach utilizes field characteristics derived from acoustic bathymetric data (such as slope and roughness at various scales) and environmental data from a hydrodynamic model (including temperature, salinity and current speed) (Mohn *et al.*, 2014; Rengstorf *et al.*, 2014). This method is commonly used to estimate favorable habitats for species or ecosystems over large unexplored areas.

For cold-water corals (CWC), probabilistic distribution models over a specific canyon region have already been applied in the northwestern Mediterranean, including the contiguous Cap de Creus Canyon (Lo Iacono *et al.*, 2018), and La Fonera/Palamós Canyon (Lastras *et al.*, 2016), as well as the Cassidaigne Canyon located in the eastern part of the Gulf of Lion (Fabri *et al.*, 2017). In the three cases, the probable distribution of the habitat has led to extending knowledge to the scale of the canyon. This knowledge of distribution makes it possible to target areas to be explored to assess CWC ecosystem status for the European Marine Strategy Framework Directive (EU, 2008b, 2017). It also supports the establishment of protection and regulation measures needed to better develop conservation plans for these species, and aids in implementing management plans and regulations to support their conservation and maintain ecosystem services.

To assess the pressure on this CWC ecosystem, particularly bottom fishing pressure, an abrasion index can be calculated using Vessel Monitoring System (VMS) data (Eigaard *et al.*, 2017). This data is primarily used to monitor the activities of fishing vessels as part of fisheries regulation and management, and provides information to government authorities or regulatory agencies. Another system, the Automatic Identification System (AIS), provides information on positioning at higher spatial resolu-

tion, and is dedicated to security at sea by enabling ships to locate each other and report their position, course and speed in order to avoid collisions and improve maritime traffic management. Global Fishing Watch (GFW), an international non-profit organization provides an interactive platform accessible on their website (https://globalfishingwatch.org/) which is a valuable tool for studying the impact of fishing on biodiversity and ecosystems (Kroodsma *et al.*, 2018).

The objective of this study is to provide decision-making support for the establishment of a strong protection zone on the Lacaze-Duthiers Canyon. To achieve this, our research integrates data on species distribution and fishing pressure, structured into three main components: (1) predictive habitat mapping of key ecosystem-engineering species (scleractinians *Madrepora oculata* and *Desmophyllum pertusum*), using seafloor variables derived from 10-m resolution bathymetry and hydrodynamic variables from an 80-m resolution hydrodynamic model; (2) the habitat characterization of each species using high-resolution (5-m) bathymetric data with the canyon head; and (3) the assessment of fishing pressure within the canyon and on the adjacent continental shelf.

Materials and Methods

Lacaze-Duthiers Canyon settings

The upper region of the Lacaze-Duthiers Canyon lies within the "Parc naturel marin du golfe du Lion", near the French-Spanish border, at the western end of the Gulf of Lion (Fig. 1). Basin circulation in this area is driven by the Northern Current, which transports warm, low-salinity waters from northeast to southwest along the margin, down to depths of 1000-1500 m (Many *et al.*, 2021). Surface velocity varies seasonally between 0.3 and 0.5 $m.s^{-1}$, decreasing to ~0.1 $m.s^{-1}$ at 200-400 m depth. Winter conditions favor the formation of dense shelf water due to cold, dry air (Mistral and Tramontane winds). These waters cascade downslope at the shelf edge, mainly via the Lacaze-Duthiers and Cap de Creus Canyons, reaching depths of up to 2000 m and velocities close to 1 $m.s^{-1}$, depending on winter severity (Canals *et al.*, 2006; Puig *et al.*, 2008; Ulses *et al.*, 2008b; Palanques *et al.*, 2012; Durrieu de Madron *et al.*, 2013). During summer, southwest Gulf of Lion currents often flow northward, generating persistent anticyclonic eddies in the mixed layer (Petrenko *et al.*, 2017). Episodic marine storms in autumn and

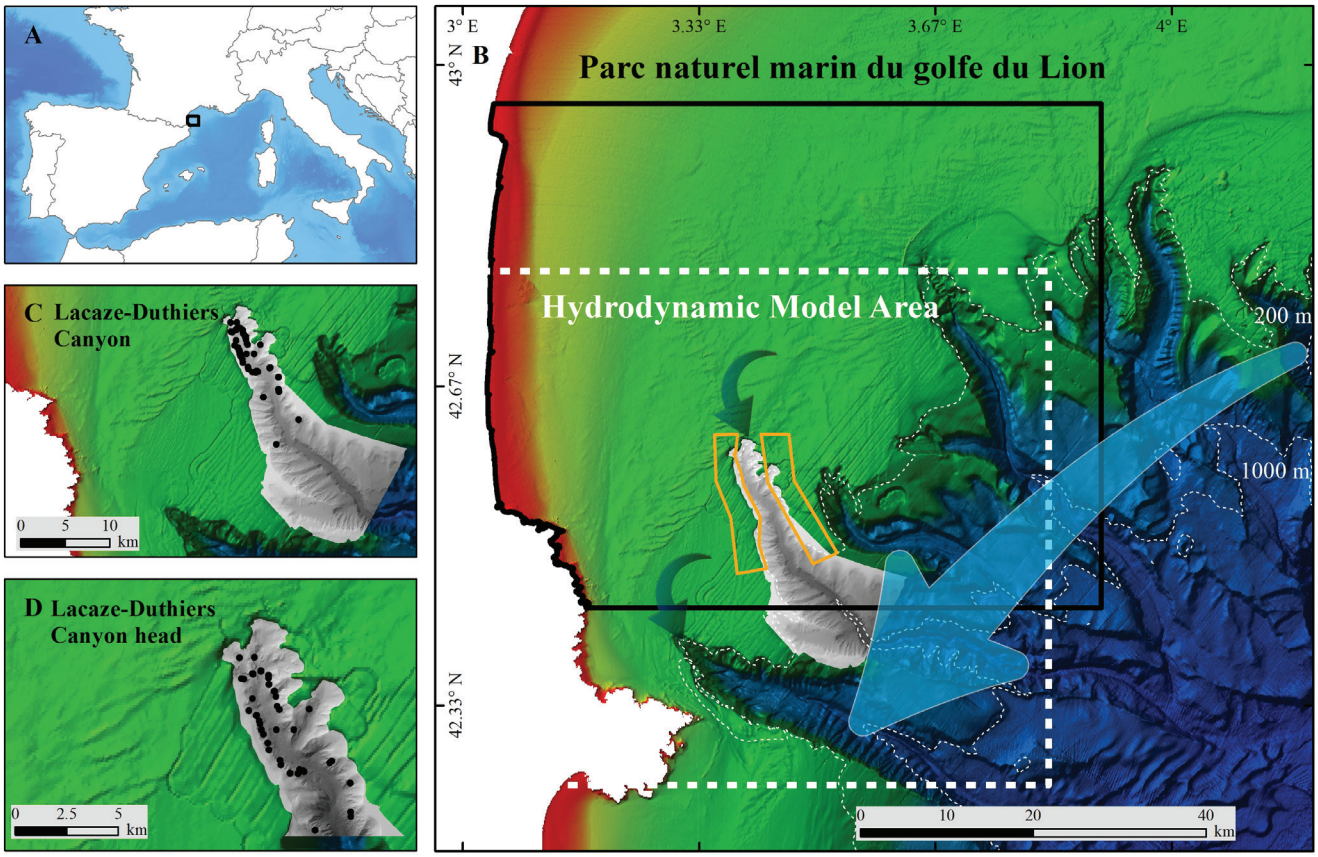

***Fig. 1*:** Map of the western Mediterranean Sea. A: Location of the "Parc naturel marin du golfe du Lion" in the northwestern Mediterranean Sea; B: Detailed map of the extent of the "Parc naturel marin du golfe du Lion" (solid black line), the domain of the hydrodynamic model used in this study (dashed white line), and the polygons used to compute the fishing effort (orange lines). The Northern Current and the dense shelf water formation areas entering the canyons are represented by light and dark blue transparent arrows; C: Area covered by the 10-m resolution bathymetric data over the upper canyon region, with location of ROV exploration dives (black dots); D: Bathymetric data at 5-m resolution over the canyon head region, with locations of ROV exploration dives (black dots).

winter cause counterclockwise along-isobath currents, accelerating southwestward due to the shelf narrowing, increasing water export (Ogston *et al.*, 2008; Ulses *et al.*, 2008a; Mikolajczak *et al.*, 2020; Estournel *et al.*, 2023). These storms resuspend fine sediments, which deposit in the canyon heads before remobilization during winter cascading events (Palanques *et al.*, 2009; Palanques *et al.*, 2012; Estournel *et al.*, 2023).

Colonial Scleractinians observation data

Data were collected in the Lacaze-Duthiers Canyon from 2009 to 2023 during several oceanographic cruises (MEDSEACAN-2009, CALADU-2019, CALADU-2021, ECALION_2023 and PLAS-SCORE-2023). Observations from 22 Comex ROV dives (Achille/Apache) and 20 Ifremer HROV dives (Ariane) were analyzed (Table S1) (Fabri *et al.*, 2025e). Coral occurrence data were extracted from ROV videos and georeferenced using Adelie software (Fabri *et al.*, 2014).

A modified CORALFISH classification (Davies *et al.*, 2017) was used to categorize coral formations, reflecting Mediterranean characteristics (Table 1). Six categories were added to the classification, excluding class 3.3.5 (undistinguishable small colonies). This classification was published before *Lophelia pertusa* was renamed *Desmophyllum pertusum*; therefore, the original name was used.

For 10-m resolution habitat modeling, *D. pertusum* and *M. oculata* were grouped, while at 5-m resolution, species were treated separately. Coral observations were used to create the species presence datasets.

Absence points were generated by identifying time periods when corals were not observed, excluding intervals when the seafloor was not visible or during the descent and ascent phases of the ROV.

Presence and absence points were scaled to match the resolution of the field data for habitat modeling. Finally, to minimize model bias, the presence and absence datasets were balanced through random sampling (Fabri *et al.*, 2025a, c, d).

Bathymetric data

Bathymetric data were collected during the CALADU-2021 expedition (doi: 10.17600/18001575) using the Kongsberg EM304 multibeam echosounder on R/V *La Thalassa*. Processed via GLOBE software (Poncelet *et al.*, 2020). To study the distribution of cold-water corals, we used a digital terrain model (DTM) of the entire canyon at the highest resolution available, i.e., 10 m {Ifremer Geo-Ocean, 2023 #2099}. The goal was to produce the broadest possible mapping of their distribution in the canyon. To characterize the habitat of each of the two species, we focused on the head of the canyon. As this area is shallower, we were able to obtain a higher-resolution DTM (5 m) {Ifremer Geo-Ocean, 2023 #2100}. This finer resolution is expected to improve our ability to distinguish between the two habitats. Only data from depths >130 m were considered, as target species are absent in shallower Mediterranean waters (Freiwald *et al.*, 2009).

Seafloor variables

Seafloor indices were derived from DTMs using the Benthic Terrain Modeler extension in ArcMap 10.7 (ESRI) including: *Slope*; *Bathy*: depth; *Aspect*:, which reflects the slope orientation; *Curvature*, which reflects water flow patterns along slopes; *Surface to Planar area*: measuring rugosity; *Vector Ruggedness Measure* (*VRM)*, measuring the dispersion of orthogonal vectors relative to

Table 1. CoralFISH Classification levels used in our study and six additional levels for Mediterranean Coral Formations. CWC: Cold-Water Corals.; Note: *Lophelia pertusa* is the former nomenclature for *D. pertusum*.

CORALFISH Classification (Davies *et al.*, 2017) and additional levels for Med. Sea	***CWC***	***D. pertusum***	***M. oculata***
1.1.1 *Lophelia pertusa* Reef	x	x	
3.1.1 Dense *L. pertusa* Framework on vertical wall	x	x	
3.3.1 Isolated colonies of *L. pertusa* on hard/mixed substrate	x	x	
3.3.2 Isolated colonies of *M. oculata* on hard substrate (vertical wall)	x		x
3.3.3 Isolated colonies of *L. pertusa* and *M. oculata* on hard substrate	x		
Dense *L. pertusa* and *M. oculata* Framework on vertical wall	x	x	x
Dense *M. oculata* Framework on vertical wall	x		x
Loosely-packed *L. pertusa* and *M. oculata* Framework on vertical wall	x	x	x
Loosely-packed *M. oculata* Framework on vertical wall	x		x
Isolated colonies of *L. pertusa* on boulders	x	x	
Isolated colonies of *M. oculata* on boulders	x		x
3.3.5 Isolated Scleractinian colonies on boulders			

the surface (computed using small resolution windows of 9, 25, and 49 pixels to minimize excessive smoothing); and *Bathymetric Position Index* (*BPI*), which captures terrain variations even at high resolutions (calculated using windows of 3, 9, 11, 25, 49, 81, and 13-123 or 25-250 pixels) (Appendix A).

Therefore, the final seafloor datasets consisted of either twelve or fifteen rasters, depending on the resolution (10 m or 5 m) (Fabri & Dreidemy, 2024b, a). The methodology is detailed and has been widely applied in previous studies (Wilson *et al.*, 2007; Mohn *et al.*, 2014; Vierod *et al.*, 2014; Bargain *et al.*, 2018).

Environmental variables

Hydrodynamic data were simulated using the numerical model SYMPHONIE (Marsaleix *et al.*, 2006; Marsaleix *et al.*, 2009) with a domain covering 65 × 60 km at 80-m horizontal resolution (Fig. 1B). The bathymetry used in the model was the "Golfe du Lion - Côte d'Azur DTM" (https://dx.doi.org/10.17183/MNT_MED100m_GDL_CA_HOMONIM_WGS84) at a resolution of 0.001° (~111 m). Locally, in the Lacaze-Duthiers Canyon, the 10-m resolution bathymetry described above was used. Vertically, the vanishing quasi-sigma (VQS) coordinate adapted to steep bathymetric slopes (Estournel *et al.*, 2021) with 50 levels in the deepest zones and 37 levels at 500 m depth was used. Atmospheric forcing was calculated using bulk formulas based on hourly outputs from the European Center for Medium Range Weather Forecasts. At the open lateral boundaries, the model was forced by daily outputs from the SYMPHONIE model applied to the entire Mediterranean, with a resolution of ~1.9 km over the Gulf of Lion (Estournel *et al.*, 2021) which was validated against temperature and salinity observations. The high resolution model was run between November 1, 2012 and April 15, 2014, covering two contrasting winters, with winter 2012-2013, being a cold winter and winter 2013-2014 a warm winter (Mikolajczak *et al.*, 2020). The first winter was characterized by cascading in the Lacaze-Duthiers Canyon down to 1000 m depth, while during the second winter, no cascading was observed at 500 m depth (Durrieu de Madron, pers. comm.). These observations are consistent with our simulation results: during the first winter, currents modeled inside the canyon approach 1 m/s, whereas in the second winter, current velocities do not exceed 0.2 m/s (see also Appendix D). These results further support the ability of the SYMPHONIE model to reproduce cascading processes in the southwestern Gulf of Lion, as previously demonstrated in Ulses *et al.* (2008), Mikolajczak *et al.* (2020), and Estournel *et al.* (2023).

Bottom currents were calculated from the first two levels above the bottom to ensure flow continuity (Estournel *et al.*, 2021). In practice, these currents correspond to depths of 7.5 m and 12 m above the bottom for total water depths of 200 m and 300 m, respectively. The selection of hydrodynamic parameters was based on current ecological knowledge of CWCs. In the Mediterranean Sea, CWCs live near their upper thermal tolerance, making temperature a key factor for their distribution. Although CWCs can tolerate high temperatures, long-term exposure can be detrimental; they rely on periods of lower temperatures to recover. Therefore, we considered temperature amplitude as a potentially relevant variable. Salinity was included for its influence on water density, which may affect larval dispersal. Currents were considered due to their complex role: moderate flows facilitate food delivery, while very weak currents may lead to sediment accumulation and smothering, and strong currents can help keep colonies clear of sediments. Horizontal components of bottom current velocities, temperature, and salinity were saved at hourly resolution., For each grid point, the 1st and 99th percentiles were extracted for salinity and temperature to produce the following files: low and high bottom salinities (*S01*, *S99*), low and high bottom temperatures (*T01*, *T99*). For current velocities, the 95th and 99th percentiles were extracted to produce files representing high and extremely high bottom current velocities (*UV95*, *UV99*). Strictly speaking, the tangential bottom current would have been more relevant than the horizontal current, which is the model's state variable. However, as the difference between the horizontal and tangential currents was less than 5%, this correction was not taken into account. These hydrodynamic variables were provided as gridded data files with a regular spacing of 80 m for each of the six variables (Estournel & Fabri, 2025). Datasets were interpolated at 5-m and 10-m resolutions. The natural neighbor interpolation method was applied, ensuring that no new values were created outside the range of existing data. Additionally, salinity and temperature amplitude rasters (*Ampli-T ; Ampli-S*) were created by subtracting *T01* from *T99* and *S01* from *S99* (Appendix A). As a result, the final hydrodynamic dataset consisted of eight rasters for each resolution (10 m or 5 m) (Fabri & Estournel, 2024a, b).

Habitat models and statitical analyses

A preliminary step was to identify correlated variable groups at each presence pixel to select a single proxy per group. Values were extracted from raster cells containing a presence point. Due to non-normal data distribution (Shapiro-Wilk test), Spearman's rank correlation was used. Hierarchical clustering (Ward's method, dissimilarity threshold = 4) was applied to define variable groups (Bargain *et al.*, 2018). To retain only the most informative predictor from each cluster, we fitted a series of candidate models in which alternative representatives of each group of correlated-variable were systematically substituted. Model selection was guided by Area Under the Curve (AUC) maximisation, with the combination achieving the highest cross-validated AUC ultimately providing the final set of predictors. The variable-selection procedure was applied independently to each species, so the final set of predictors reflects both the ecological niche and the statistical properties of the data for that particular taxon (Table 2).

Table 2. List of variables used and their contributions to the habitat models constructed using the two methods in the three configurations considered: without species distinction at a 10-m resolution, *D. pertusum* at a 5-m resolution and *M. oculata* at a 5-m resolution. *UV99*: High bottom current velocity; *Ampli-T*: Temperature Amplitude; *BPI03*: Bathymetric Position Index at 3-pixel resolution; *T99*: High bottom temperature; *S01*: Low bottom salinity. CWC: Cold-Water Corals.

	CWC 10 m		*D. pertusum* 5-m		*M. oculata* 5-m	
Prevalence	0.24		0.11		0.17	
	Maxent	*GAM*	*Maxent*	*GAM*	*Maxent*	*GAM*
Slope (%)	52.9	52	52.3	28	81.5	54
UV99 (%)	24.8	26	31.9	52	0.9	15
Ampli-T (%)	22.3	22	14	17		
BPI03 '%)			1.8	3		
T99 (%)					14.7	22
S01 (%)					2.9	8
AUC Validation (%)	95	82	94.2	85	94	82

Box plots and non-parametric Kruskal-Wallis tests were used to compare variables across the three coral presence datasets: grouped and separated *D. pertusum* and *M. oculata* species. Dunn's test with Bonferroni correction were used to identify significant differences.

Habitat models were developed using Generalized Additive Models (GAM) (Biomod2 R package) and Maximum Entropy Modeling (MaxEnt). GAM relies on both presence and absence data. In our case, the absence data used were true absences, identified along ROV tracks, as described in the observation data section.

Generalized Additive Modeling (GAM) is a flexible, non-linear extension of Generalized Linear Models (GLM), allowing for complex relationships between predictors and response variables (Wood, 2017). GAM uses smooth functions to model the relationship between environmental variables and species occurrence (presence/absence data), which helps capture intricate patterns in the data, such as non-linearities and interactions between predictors. This flexibility makes GAM particularly suited for ecological data, where species-environment relationships are often non-linear (Guisan *et al.*, 2002). The Generalized Additive Model (GAM) algorithm was implemented using the Biomod2 package (version 4.2-4) in R (Thuiller *et al.*, 2009).

Maximum Entropy Modeling (MaxEnt) is based on the relationships between variables at the species' presence points, employing a maximum entropy approach. This method identifies constraints that the species distribution must satisfy and selects the models with the highest Shannon entropies (Phillips *et al.*, 2006; Elith *et al.*, 2011). MaxEnt is particularly useful when data are limited (Phillips *et al.*, 2006; Baldwin, 2009; Elith *et al.*, 2011). The MaxEnt algorithm was used with selected Hinge features, a regularization multiplier of 2, and all other parameters set to their default values.

Both models used cross-validation (100 repetitions, 70% training, 30% validation), with variable importance assessed via 10 permutations. Model performance was evaluated using the AUC, where values above 0.7 indicate acceptable predictive power (Elith *et al.*, 2011).

Fishing pressure data

The SAR abrasion index, represents the swept surface area calculated by multiplying the linear extent of fishing activity by the width of the fishing gear (Georges *et al.*, 2021). The linear extent of fishing activities was estimated using data from the VMS installed on all vessels over 12 meters in length. This estimation distinguishes periods of active fishing from navigating (Ifremer, 2021). These data were aggregated into 1' arc cells (1365 m at 42º 30' latitude), and the width of fishing gear was derived from vessel and gear characteristics (Eigaard *et al.*, 2017; Georges *et al.*, 2021). The swept area is then expressed relative to the cell surface (hence the area ratio) and illustrates the number of times the cell is swept by bottom contacting fishing gear by unit of time (here over one year). Fishing gears like longlines and gillnets are excluded from the SAR calculation because their width cannot be incorporated. Annual maps of this index in French waters are available on Sextant (Ifremer, 2024).

The Apparent Fishing Effort (AFE) data, derived from AIS data, provided by GFW (https://globalfishingwatch.org/) report apparent fishing hours by gear type and vessel nationality, derived from vessel speed and directional changes (Kroodsma *et al.*, 2018). To analyze these data, we defined two polygons of approximately the same area (~47 km²) on the western side and eastern side of the canyon, above 200m depth. The polygons were created as wgs84 shapefiles and compressed into zip files to be loaded into the GFW platform. This process allowed us to retrieve annual time spent fishing in each polygon

from the GFW platform. The retrieved data include apparent fishing hours per active vessel, along with its flag and gear type. Extracted data were pre-processed: fishing hours attributed to gears such as purse seines and drifting longlines (targeting pelagic species) were excluded, retaining only bottom-contact fishing gears (e.g., trawlers and fixed gears, including gillnets and longlines).

Data from 2020 to 2023 were aggregated to assess cumulative pressure on deep-sea ecosystems, characterized by very slow growth rates.

Observations of in situ fishing impacts

Video and photographic observations obtained from ROV surveys enabled the localization of lost fishing gear within the Lacaze-Duthiers Canyon. On the continental shelf, observations were conducted using a towed camera system called Pagure. This system was deployed in 2021 during the IMPEC campaign aboard the R/V L'Europe (https://doi.org/10.17600/18001594).

Results

Occurrence of colonial scleractinians

Presence points of coral colonies, irrespective of species, were downscaled to match the 10-m bathymetric resolution, resulting in 739 presence pixels., and 3,032 absence pixels (prevalence = 0.24). Absence pixels were randomly subsampled for balance.

For species-specific habitat modeling at 5-m resolution, *D. pertusum* was represented by 504 presence pixels (prevalence = 0.11) and *M. oculata* by 768 pixels (prevalence = 0.17). Absence data (initially 4,333 pixels) were subsampled accordingly.

Variables selection and contribution to habitat models

For each coral presence dataset, a selection process based on inter-variable correlation (Hierarchical clustering, Ward's method, Spearman correlation) and AUC performance (AUC maximization) was conducted to obtain a final subset of predictors (Appendix A). This variable selection procedure was applied independently to each taxon, so that the resulting predictor sets reflect the specific ecological niche and data structure associated with each case (Table 2).

Three predictor variables were used at 10-m resolution for CWC: *Slope*, *UV99*, and *Ampli-T*. For *D. pertusum* at 5-m resolution, the variables were *Slope*, *UV99*, *Ampli-T*, and *BPI03*, whereas for *M. oculata* at the same resolution, they were *Slope*, *UV99*, *T99*, and *S01* (Appendix A; Table 2).

Maps of selected variables are shown in Figure 2, and variable contributions appear in Table 2.

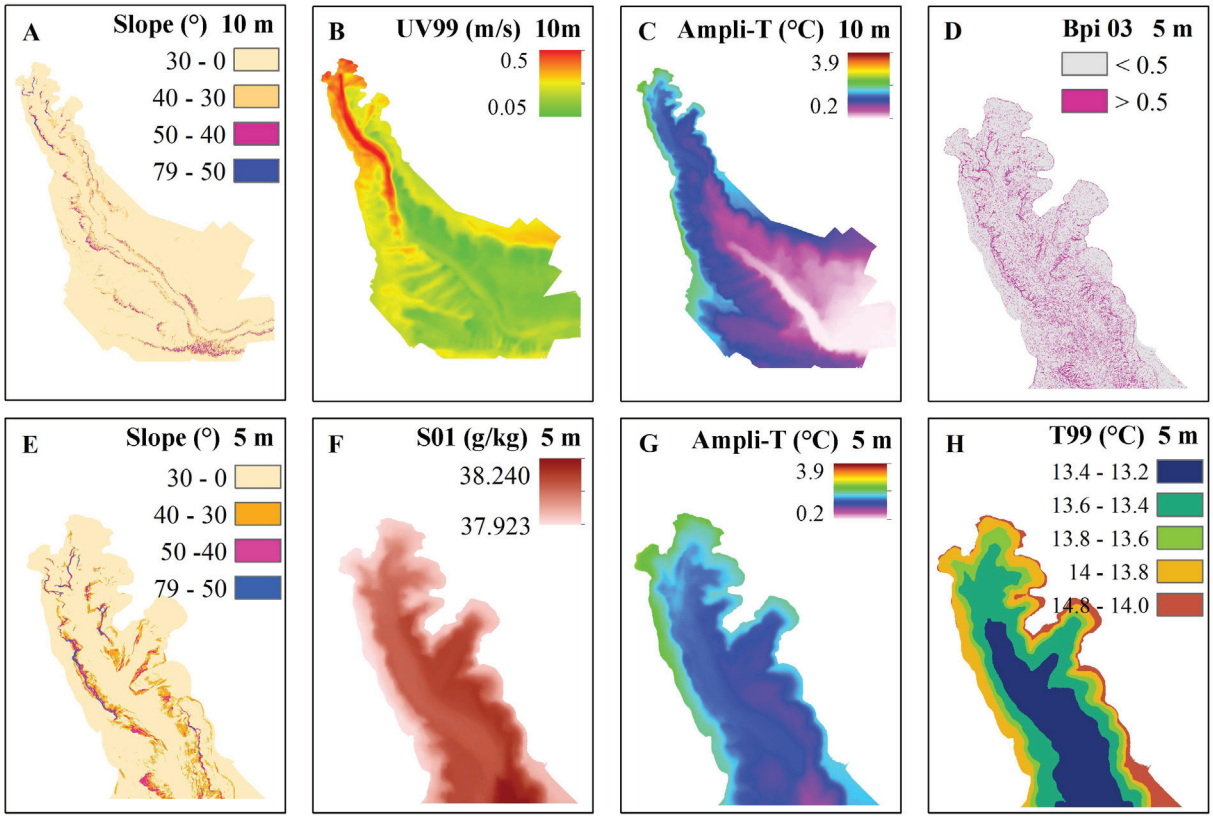

Fig. 2: Distribution of variables in the Lacaze-Duthiers Canyon. At the global scale with 10-m resolution: A: *Slope*; B: *UV99* (High bottom current velocity); C: *Ampli-T* (Bottom Temperature Amplitude). At the scale of the canyon head with a 5-m resolution: D: *BPI03* (Bathymetric Position Index at 3-pixel resolution); E: *Slope*; F: *S01* (Low bottom salinity); G: *Ampli-T* (Bottom Temperature Amplitude); H: *T99* (High bottom temperature).

Box Plots and Response curves for variables

Box Plots illustrate environmental conditions where the species were observed (Fig. 3). *M. oculata* occurs on steeper slopes (~60%), while *D. pertusum* is found on both gentle and steep slopes. *Desmophyllum pertusum* prefers higher current velocities (~0.45 m/s), while *M. oculata* tolerates moderate currents (~0.25 m/s). Ampli-T values are centered ~1.4°C for both species, but *M. oculata* favors the highest T99 (~13.5°C) while high temperature did not significantly constrain *D. pertusum* over the studied domain. Positive *BPI03* values suggest preference for elevated structures at the scale of 3 pixels, for both species, corresponding to 30 m at the global scale of the canyon and 15 m at the scale of the canyon head. Both species live at locations where low bottom salinity is centered ~38.1.

Statistical tests (Kruskal-Wallis, Dunn test) confirmed significant differences between groups ($p < 0.05/2$), except for Ampli-T values (CWC vs. *D. pertusum*) indicated by the letter 'a' in Figure 3.

Response curves illustrate how the predicted probability of presence varies in relation to each environmental variable, while holding all other variables constant at their mean sample values (Fig. 4). These curves provide insight into the individual influence of each variable on species' habitat suitability.

In our models, response curves show that habitat suitability increases with *Slope* and *UV99* until stabilizing (Fig. 4). For *D. pertusum*, suitability declines when *UV99* > 0.5 $m \cdot s^{-1}$ with Maxent (Fig. 4), while it stabilizes with GAM (Appendix B). *Ampli-T* peaks at ~1.4°C, with *D. pertusum* showing an artifact-related secondary peak which does not reflect a realistic ecological response to temperature variations, possibly due to statistical interference with another variable. *Madrepora oculata* shows a *T99* peak at 13.5°C. *BPI03* effects are minimal (~2% contribution). *S01* shows unrealistic response patterns with a depression in the middle, but contributes only 3% with Maxent and 8% with GAM (Table 2).

Model Validation

AUC scores exceeded 80% across all cases, with Maxent consistently above 94% (Table 2). We assessed performance and robustness using multiple validation methods. Low omission rates indicate few missed presences. The calibration curves show good agreement between predicted probabilities and observed data, confirming reliable estimates. K-fold cross-validation demonstrated stable performance across data subsets. Sensitivity-specificity tests revealed a balanced compromise between true positive and true negative rates, supporting accurate classification. Jackknife tests highlighted key predictors and confirmed model robustness. Overall, these results indi-

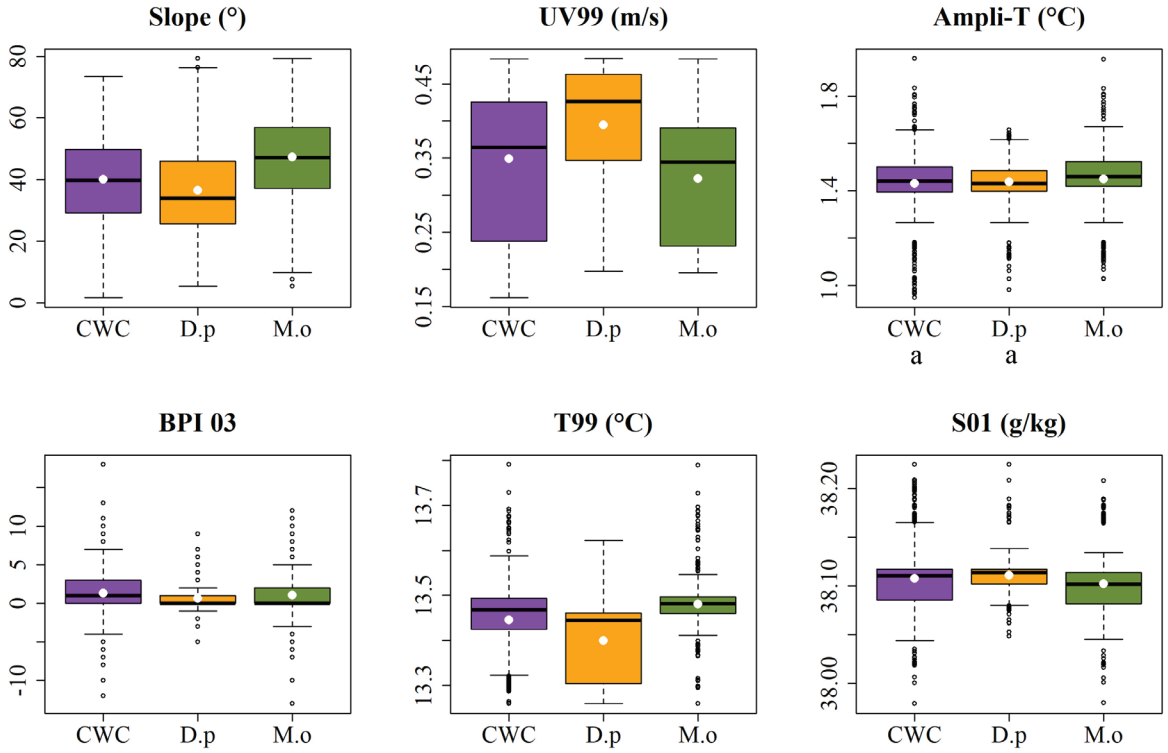

***Fig. 3*:** Box Plots of non-correlated variables used to build Maxent and GAM distribution models. The boxplots display the median as a horizontal line inside the box. The box represents the interquartile range (Q3-Q1), with whiskers extending to the most extreme non-outlier values. Outliers are shown as individual points. The mean (white dot) has been added for reference. The letter 'a' indicates no significant difference between groups. *UV99*: High current velocity; *Ampli-T*: Temperature Amplitude; *BPI03*: Bathymetric Position Index at 3-pixel resolution; *T99*: High bottom temperature ; *S01*: Low bottom salinity. CWC: Cold-Water Corals ; D.p.: *D. pertusum*; M. o.: *M. oculata.*

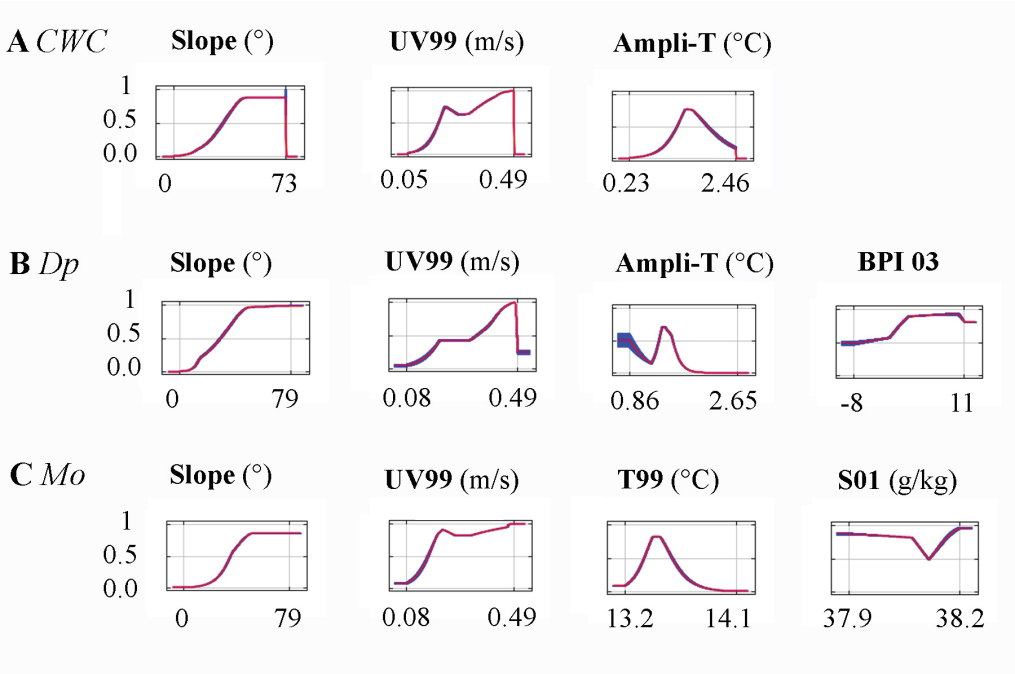

Fig. 4: Response curves showing Maxent prediction for each variable; the blue shading represents the confidence interval. A: for CWC at the canyon scale with a 10-m resolution. B: for *D. pertusum* at the canyon head with a 5-m resolution; C: for *M. oculata* at the canyon head with a 5-m resolution. *UV99*: High current velocity; *Ampli-T*: Temperature Amplitude; *BPI03*: Bathymetric Position Index at 3-pixel resolution; *T99*: High temperature ; *S01*: Low bottom salinity. CWC: Cold-Water Corals; D.p.: *D. pertusum*; M. o.: *M. oculata.*

cate that all the models perform well and provide reliable predictions (Appendix B, C).

Probable habitats

The probable habitats predicted at the scale of the upper canyon region, with a 10-m resolution, are primarily located on the western flank in the canyon head (Fig. 5A). The GAM method predicts probable zones in the southern part of the canyon, even where no *in situ* data are available. Maxent, on the other hand, limits its predictions to areas where presence data have been observed and consistently predicts probable habitats at shallower depths compared to GAM. The probable habitat common to both models, shown in black in Figure 5, represents intermediate zones in terms of depth and latitude. In all cases, the probable habitats predicted by both methods overlap.

When examining habitats in the canyon head at a 5-m resolution, the distribution of *D. pertusum* habitat closely aligns with the predicted distribution at 10-m resolution for both species combined (Fig. 5B). In contrast, the *M. oculata* habitat is distributed on both sides of the canyon head, primarily along the continental shelf break and the upper canyon flanks (Fig. 5C).

When comparing probable habitat areas (Table 3), the area predicted at a 10-m resolution is larger than that predicted at a 5-m resolution. Additionally, the habitat area predicted for *D. pertusum* is larger than that predicted for *M. oculata* (Table 3). It is also evident that the Maxent method consistently predicts smaller habitat areas compared to the GAM method, while the overlap between areas predicted by both methods is approximately the same as the area predicted by Maxent (Table 3).

Table 3. Probable habitat areas estimated by each method for the three case studies, considering suitability greater than 70%. CWC: Cold-Water Corals

	Area suitable for both CWC species, at 10 m resolution		Area suitable for *D. pertusum*, at 5 m resolution		Area suitable for *M. oculata*, at 5 m resolution	
	Nb of 10 m pixels	Area (km²)	Nb of 5m pixels	Area (km²)	Nb of 5m pixels	Area (km²)
Maxent	15082	1.50	40514	1.01	24393	0.61
GAM	34742	3.47	99712	2.49	54783	1.37
Intersection	13543	1.35	37301	0.93	22170	0.55

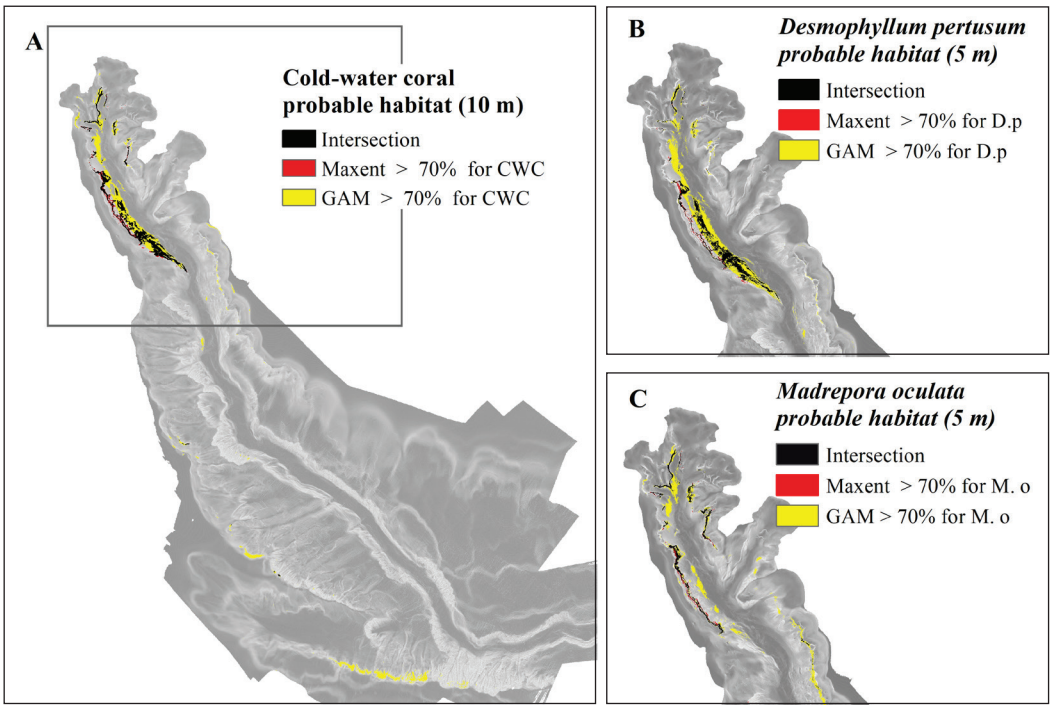

Fig. 5: Distribution maps of probable habitats calculated using the Maxent and GAM methods. Pixels predicted as probable habitats with a suitability greater than 70% by both methods are shown in black. A: CWC without distinction, combined at 10-m resolution; the black rectangle indicates the extent of the 5-m resolution models; B: *Desmophyllum pertusum* at a 5-m resolution; C: *Madrepora oculata* at a 5-m resolution.

Habitat Characteristics

The habitats of both species are distinct due to their depth distribution: *D. pertusum* is generally found at greater depths than *M. oculata* (Fig. 6). Nevertheless, both species can be found together along the canyon flank, where the terrain is not smooth but instead forms nooks and crannies (Fig. 7).

In addition, *D. pertusum* is primarily seen located on gentler slopes at the base of cliffs, whereas *M. oculata* tends to occur on steeper slopes, where lithified sedimentary strata outcrop.

Distribution maps of fishing impact data

Average SAR data in the "Parc naturel marin du golfe du Lion", based on VMS data over a 4-year period, from 2020 to 2023, indicate significant abrasion pressure, primarily concentrated near the coast (Fig. 8). Global fishing pressure decreases progressively across the shelf, as distance from the coast increases, being minimum (SAR = 2 to 4) near the continental shelf break (Fig. 8). This suggests that the surface of seabed area swept by bottom-contact fishing gear in these cells is equivalent to 2 to 4 times the total surface area of the cells over the 4-year period considered.

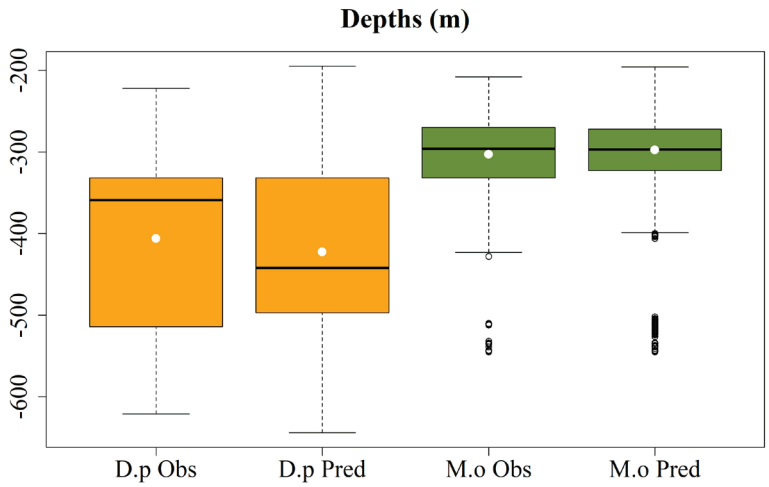

Fig. 6: Box plots showing the depth distributions of both species in the canyon, based on observed (Obs.) and model predictions (Pred.). D.p.: *D. pertusum* is shown in orange; M. o.: *M. oculata* in green. The boxplots display the median as a horizontal line inside the box. The box represents the interquartile range (Q3-Q1), with whiskers extending to the most extreme non-outlier values. Outliers are shown as individual points. The mean (white dot) has been added for reference.

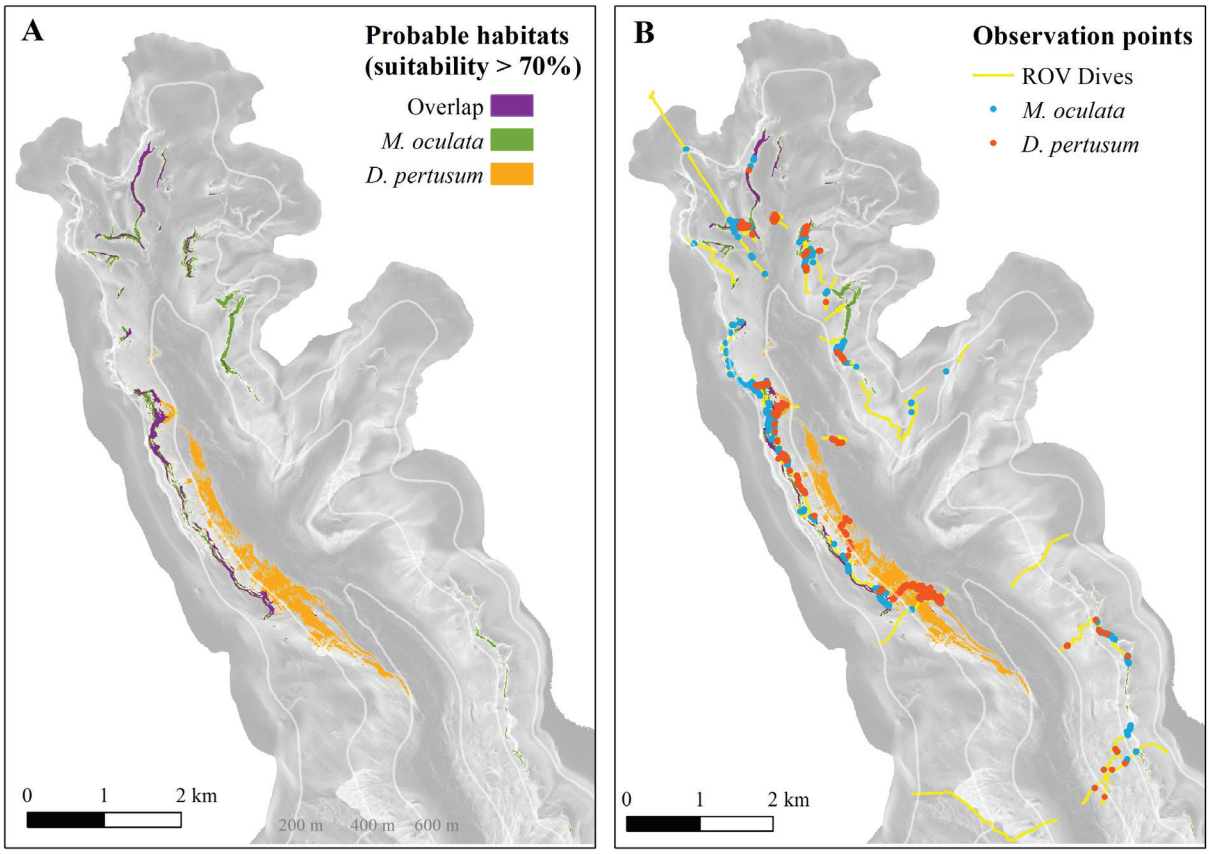

Fig. 7: Distribution maps in the Lacaze-Duthiers Canyon. A: Probable habitats for the two colonial coral species *D. pertusum* (in orange) and *M. oculata* (in green) (Fabri *et al.*, 2025b). Areas suitable for both species are highlighted in dark purple. B: Observation points of the two colonial coral species *D. pertusum* (in red) and *M. oculata* (in blue) overlapping their probable habitats.

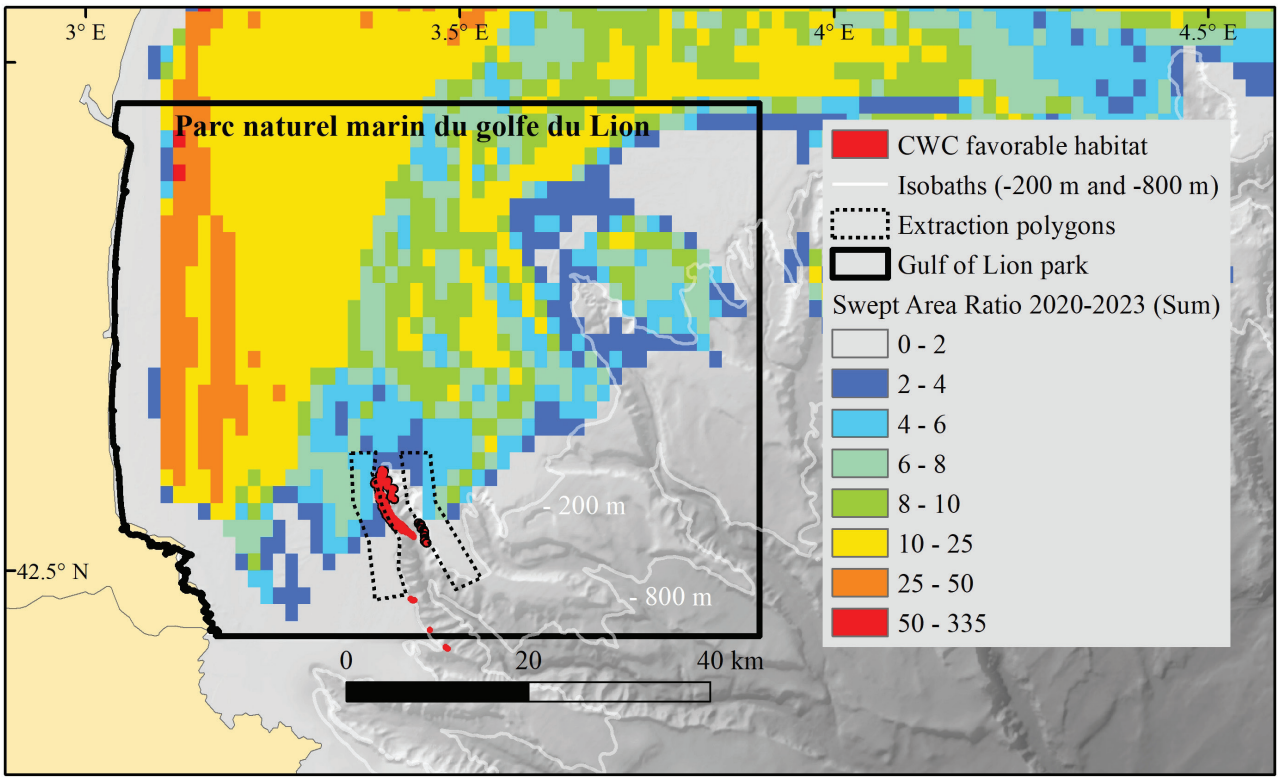

Fig. 8: Identification of fishing areas based on the SAR abrasion index derived from VMS data (sum 2020-2023), aggregated at a resolution of 1'x1'; The probable habitat of CWC is represented in red. The extraction polygons are represented as black dots on the western and eastern shelves at the edge of the canyon.

AFE, provided by GFW and derived from AIS data, highlights coastal areas heavily impacted by bottom-contact fishing (shown as white pixels in Fig. 9A), while also identifying two areas at the shelf break, on the west and east sides of the Lacaze-Duthiers Canyon head. Within the two polygons, the fishing effort from 2020 to 2023 was exclusively attributed to vessels classified as 'trawlers' in the GFW database with 99% of these vessels being from Spain (Fig. 9B). No fishing effort associated with 'fixed gears' was recorded.

As shown in Figure 9B, within the two polygons Spanish trawlers accounted for 51% of the AFE on the western shelfs and 48% on the eastern shelf regions of the Lacaze-Duthiers Canyon head. A total of 19 trawlers from Spain operated on both sides of the canyon. In addition, five trawlers focused exclusiveley on the western shelf (accounting for 37% of the western AFE), while three focused on the eastern shelf (7% of the eastern AFE). French trawlers contributed only 1% of the total AFE, with each vessel operating on either side of the canyon (Table S2).

Observation of in situ fishing impacts

Examples of lost fishing gear found in the Lacaze-Duthiers Canyon are shown in Figure 10, along with an example of a trawled seabed on the continental shelf above (Fig. 10A). Lost longlines and trawling nets have frequently been observed. Nets are often difficult to detect as they become entangled with the surrounding benthic species and only become visible upon closer inspection (Figs. 10F, 9I). Recently lost longlines are extremely difficult to see as they are very thin and therefore represent a hazard to ROVs, especially when they float in the water column (Figs. 10B, 10E ; 10H). In contrast, older longlines, already colonized by species such as corals and oysters, are more easily noticeable (Figs. 10D ; 10G ; 10J).

Lost longlines and nets were observed all around the head of the Lacaze-Duthiers Canyon, from the western to the eastern and northern edges, and also in the canyon axis (Figs. 10C ; 10F). On the contrary, no signs of trawling were observed along the axis of the canyon, nor on the flanks.

Discussion

The results of this study highlight several key aspects regarding the distribution of marine animal forests in the Lacaze-Duthiers Canyon and the anthropogenic pressures impacting this ecosystem.

Distribution of probable habitats

Probable habitat modeling combined with direct ROV observations enabled us to map the spatial distribution of colonial scleractinians throughout the upper canyon region. While the Maxent and GAM models differed regarding the extent of predicted habitats, both identified common areas with a high probability of occurrence. The distribution of the two species studied, *M. oculata* and *D. pertusum*, is not homogeneous. *Desmophyllum pertusum* is predominantly found at greater depths and on gentler slopes at the base of cliffs, while *M. oculata* is more frequently observed at shallower depths, on steep slopes, and on outcroped lithified sedimentary strata. These findings align with previous localized observations (Fabri *et al.*,

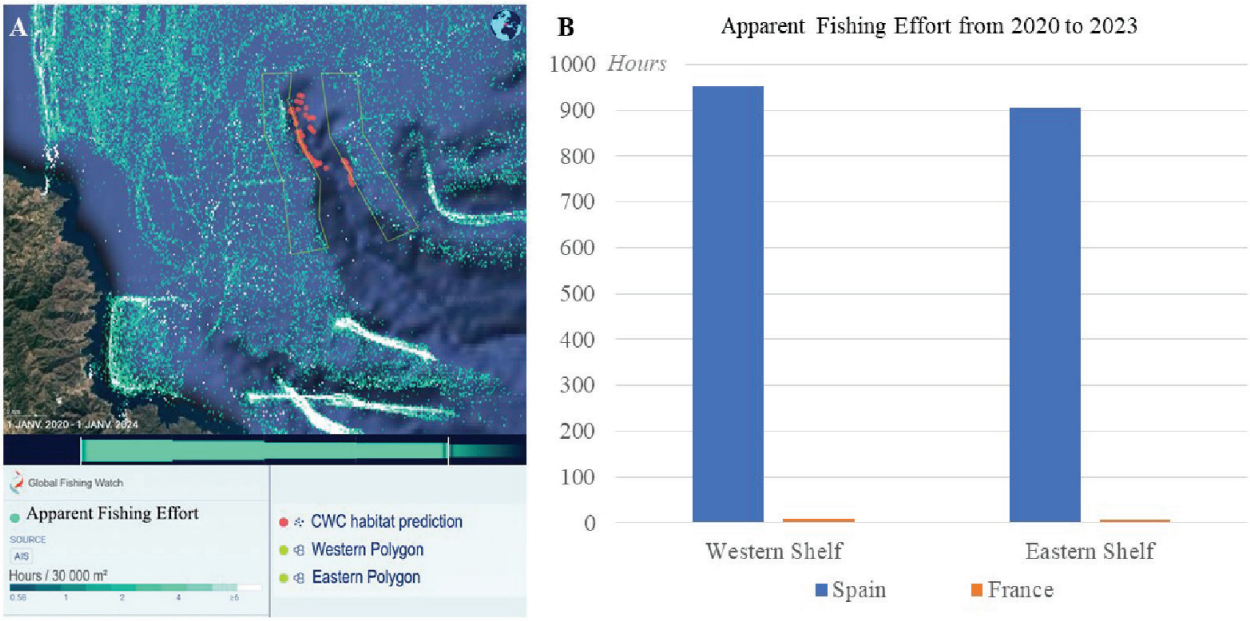

Fig. 9: Identification of fishing areas using the AFE provided by GFW, derived from AIS data (sum 2020-2023 and expressed in hours per unit area. A: The probable CWC habitat is represented in red, and extraction polygons are represented as green lines on the western and eastern shelves at the edge of the canyon. B: Histograms showing the AFE carried out by trawlers from 2020 to 2023, within the selected polygons on the western and eastern shelf regions of the Lacaze-Duthiers Canyon head. The data is categorized by vessel flag (Spain in blue and France in orange).

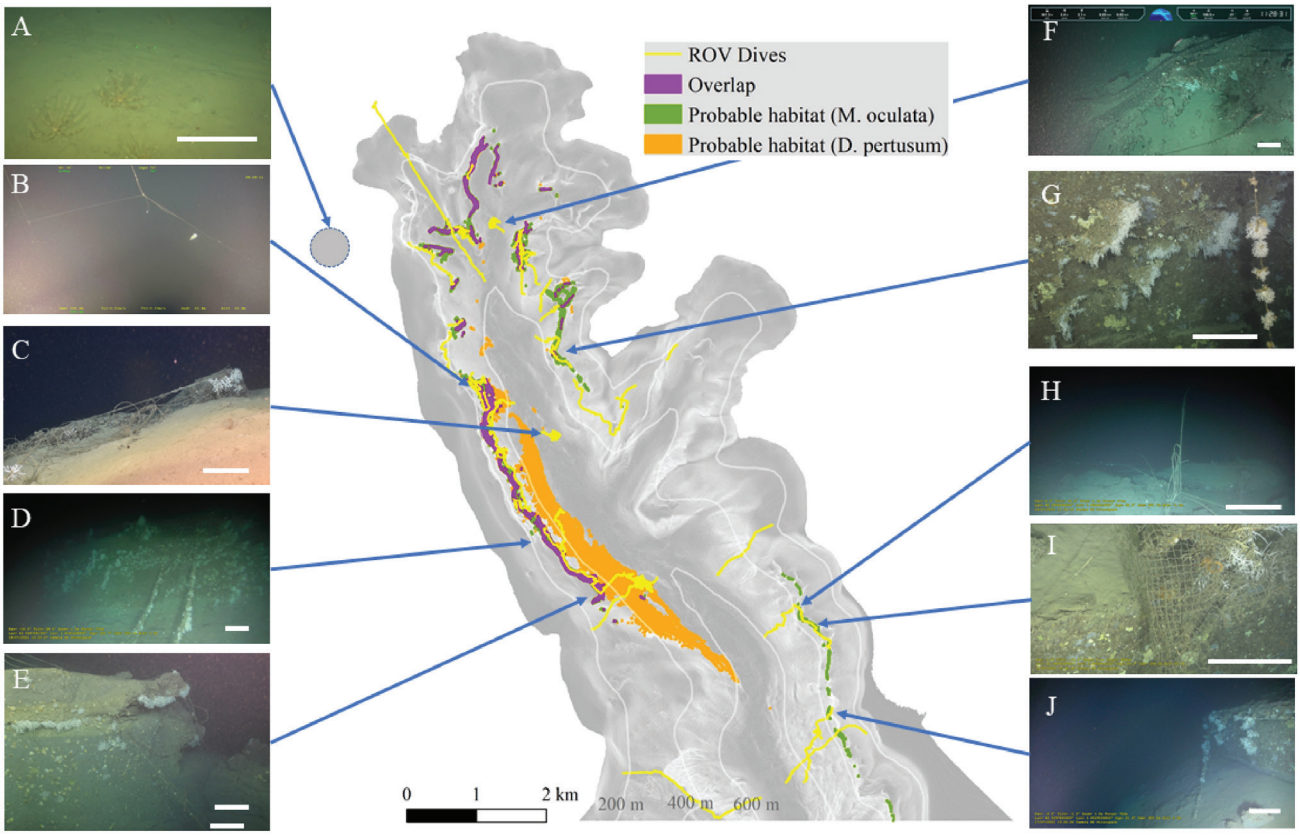

Fig. 10: Fishing impact images from the Lacaze-Duthiers Canyon. Scale bar: ~50 cm. A: Trawling track observed on the continental shelf near the canyon head (100 m depth), IMPEC_2021, Pagure Station 9C; B: Recently lost longline on the flank with a fish caught on a hook, CALADU_2019, Ariane PL 145-07 (270 m); C: Recently lost longline in the canyon axis, PLAS-SCORE-2023, Ariane PL 257-04 (495 m); D: Old longline, on the western flank, CALADU-2021, Ariane PL 193-08 (320 m); E: Recently lost longline on the western flank, CALADU-2021, Ariane PL 190-05 (283 m); F: Trawlnet in the head of the canyon, PLAS-SCORE-2023, Ariane PL 256-03 (361 m); G: Old longlines on the eastern flank, CALADU-2021, Ariane PL189-04 (302 m); H: Recently lost longline on the eastern flank, CALADU-2021, Ariane PL 191-06 (303 m); I: Trawlnet on the eastern flank, CALADU-2021, Ariane PL 191-06 (300 m).

2022). Moreover, the two species seem to coexist in areas where topographical features generate turbulence and promote the retention of suspended particulate organic matter transported by currents (Fabri *et al.*, 2022). These areas, often located along canyon flanks, are of particular ecological significance as they support high abundance and biodiversity.

Distribution of M. oculata

The colonial scleractinian *M. oculata* is one of two species present in the Mediterranean capable of forming bush-like structures (Zibrowius, 2003). Its distribution in the Mediterranean is broader than that of *D. pertusum* (Freiwald *et al.*, 2009; Canals *et al.*, 2019).

In the Lacaze-Duthiers Canyon, *M. oculata* is primarily found on rocky outcrops and steep slopes, consistent with findings in Spanish submarine canyons, where slope was also a key factor in the Cap de Creus Canyon (Lo Iacono *et al.*, 2018) and in the La Fonera/Palamós Canyon (Lastras *et al.*, 2016). Recently, it has been observed in the Blanes Canyon, mainly on vertical walls at the canyon head (Bilan *et al.*, 2025). In contrast, in the Cassidaigne (eastern Gulf of Lion) and Bari (Adriatic Sea) canyon terrain irregularities played a major role in its distribution (Fabri *et al.*, 2017; Bargain *et al.*, 2018).

Apart from *Slope*, *UV99* and *T99* alsoinfluence *M. oculata* distribution in the Lacaze-Duthiers Canyon, as seen in the Cassidaigne Canyon, where models also confirmed the influence of high temperature and current (Fabri *et al.*, 2017). In the Bari Canyon, however, mean current velocity and mean temperature were more significant (Bargain *et al.*, 2018). Unfortunately, hydrodynamic data were not considered in studies of the Cap de Creus and La Fonera/Palamós submarine canyons, where only terrain parameters such as orientation and roughness were analyzed (Lastras *et al.*, 2016; Lo Iacono *et al.*, 2018).

A global study on 10 CWC species, including *D. pertusum* and *M. oculata*, produced species distribution models at 500 m resolution (Tong *et al.*, 2023). Both species were well-represented in the Mediterranean Sea, with *M. oculata* showing a wider distribution than the other species. This suggests that *M. oculata* may have a greater tolerance to environmental conditions encoutered in the Mediterranean Sea and potentially a greater resilience to climate change (Tong *et al.*, 2023). The study also underscored the importance of high-resolution environmental data to avoid masking habitat variations (Tong *et al.*, 2023).

This broader distribution and apparent resilience align with experimental findings on temperature effects at the holobiont level, showing *M. oculata* is more resistant to temperature variations than *D. pertusum* (Chapron *et al.*, 2021).

Distribution of D. pertusum

The predicted distribution of *D. pertusum*, the main reef-building species, in the Lacaze-Duthiers Canyon, is primarily influenced by *Slope* and *UV99*. However, the relative importance of these factors varies depending on the algorithm used (GAM or Maxent). A third parameter, *Ampli-T*, also plays a role in shaping this species' distribution.

As illustrated in Figure 2, *Ampli-T* and current velocity are higher on the western flank, where *D. pertusum*is concentrated (Fig. 7), particularly in areas with an *Ampli-T* ~ 1.4°C and high current velocity ~0.5 $m.s^{-1}$. High *Ampli-T* is associated with cascading events, during which cold shelf water rapidly plunges into the canyon, generating strong currents and temperature drops and increased sediment suspension(Ogston *et al.*, 2008). In the Lacaze-Duthiers Canyon, severe cascading can cause temperature drops of 3°C and currents up to 1.25 $m.s^{-1}$ (Durrieu de Madron *et al.*, 2013), more regular events decrease temperatures of 0.5 to 1°C and produce currents up to 0.6 $m.s^{-1}$ (Palanques *et al.*, 2006b; Durrieu de Madron *et al.*, 2013). These parameters are considered critical for coral survival, since strong currents prevent their burial under enhanced sedimentary deposition (Palanques *et al.*, 2009). Additionally, during cascading events, the particulate organic matter advected by currents from coastal and shelf environments provides nutritive particles to these benthic suspension feeders (Sanchez-Vidal *et al.*, 2009; Pasqual *et al.*, 2010), presumably promoting coral colony growth (Chapron *et al.*, 2020b). Maintaining cold temperatures during and after cascading events is also essential, as Mediterranean CWCs live near their upper thermal limit (Brooke *et al.*, 2013; Lunden *et al.*, 2014). When temperatures exceed 15°C, both coral species show signs of declining health, such as reduced growth, diminished energy reserves, and increased proliferation of opportunistic bacteria (Chapron *et al.*, 2021).

To date, *D. pertusum* habitat, modeled independently of *M. oculata*, has not been studied in other Mediterranean submarine canyons, although its presence is documented in several (Freiwald *et al.*, 2009; Fink *et al.*, 2015; Canals *et al.*, 2019; Bilan *et al.*, 2025). A large-scale model(230 m resolution) identified submarine canyons and continental slopes of the Mediterranean as favorable habitats for *D. pertusum* (Matos *et al.*, 2021). At this resolution, the presence of submarine canyons incising into the continental slopes and shelves can be resolved, leading to the identification of most canyons as probable zones for *D. pertusum* occurrence (Matos *et al.*, 2021). However, not all canyons host CWCs, as larvae require hard, clean substrates for successful settlement (Vertino *et al.*, 2010). Thus, large-scale assessments remain imprecise due to discontinuous hard substrates not properly mapped at wide-scale (Puig & Gili, 2019), highlighting the need for finer-scale studies.

In the Northeast Atlantic, predictive models for the Whittard Canyon have shown that incorporating hydrodynamic data improves CWC habitat predictions (Pearman *et al.*, 2020). These models suggest that CWC occurrence increases with topographic complexity and bottom currents up to 0.25 $m.s^{-1}$, as moderate currents enhance food delivery, while excessive ones prevent prey capture (Orejas *et al.*, 2016) and colony extension (Chapron *et al.*, 2020b). Our study aligns with these findings. The high current response curves for *D. pertusum* indicate that excessively strong currents exceeding ~0.5 $m.s^{-1}$ are unfavorable for this species (Fig. 4). This is supported by *in situ* experiments in the showing reduced linear colony extension, although polyp budding remains high, during periods with severe dense shelf water cascades (Chapron *et al.*, 2020b). In contrast, the presence of *M. oculata* stabilizes at high current values (>0.5 $m.s^{-1}$), showing no decline (Fig. 4). This difference in current tolerance may explain the distinct distributions in the canyon.

Data from the SYMPHONIE hydrodynamic model

The hydrodynamic variables used in our study, derived from the SYMPHONIE hydrodynamic model, span a period of over a year (November 2012 - April 2014), thus encompassing two winters. During this time frame, a major cascading event was observed in 2013 (Durrieu de Madron *et al.*, 2023). This cascading was modeled and incorporated into the analyzed data (Estournel *et al.*, 2023).

The second hydrodynamic variable introduced in our models, after the high current velocity (*UV99*), is related to temperature. More specifically, high temperature (*T99*) was used for *M. oculata*, while *Ampli-T* was selected for *D. pertusum*. It is important to note that these variables were chosen as proxies representing a group of correlated parameters. High temperature (*T99*) highlights the shallower areas of the canyon, where warmer waters overlay colder ones, whereas Ampli-T identifies regions within the canyon experiencing the most significant thermal variations, typically associated with cascading events. These areas, primarily located along the western flank of the canyon head, notably correspond to zones with the strongest bottom currents, indicating highly energetic regions (see Appendix D for current directions).

However, the *Ampli-T* raster was derived by subtracting two layers (*T99* and *T01*) at a resolution of 5 or 10 meters, depending on the case study. The initial spatial resolution of the hydrodynamic model was 80 m. To integrate these data into our distribution models, they were interpolated to a finer resolution of 10 m or 5 m. While this interpolation provided the necessary detail, it also introduced smoothing, making the interpolated data less precise than seafloor variables derived directly from bathymetric data collected at a 10-m resolution. Enhancing the spatial resolution of hydrodynamic data, however,

could improve the accuracy of our distribution models (Pearman *et al.*, 2020; Tong *et al.*, 2023).

Habitat surface areas

The predicted CWC habitat in the Lacaze-Duthiers Canyon, regardless of species, ranges between 1.3 km² and 3.5 km², depending on whether we consider the overlap between two models or the output of a single model.

Compared to the Cassidaigne Canyon, on the eastern end of the Gulf of Lion, the Lacaze-Duthiers Canyon harbors significantly larger habitats. In the Lacaze-Duthiers Canyon, *M. oculata* habitats cover between 0.6 km² and 1.4 km², versus only 0.001 km² in the Cassidaigne Canyon, where *D. pertusum* is completely absent (Fabri *et al.*, 2019).

In adjacent canyons in the western Gulf of Lion, *M. oculata* is also predicted on the steep slopes of the western flank of the Cap de Creus Canyon (Lo Iacono *et al.*, 2018), and at tributariy heads in the La Fonera/Palamós Canyon (Lastras *et al.*, 2016). However, no surface area was reported for *M. oculata*, and no predicted habitat map was generated for *D. pertusum* due to the scarcity of its colonies.

When examining each species separately within the Lacaze-Duthiers Canyon, the habitat favorable to *D. pertusum* is more extensive (1.0–2.5 km²) than that of *M. oculata* (0.6–1.4 km²). Consequently, *D. pertusum* accounts for 64% of the total habitat area, while *M. oculata* represents 36%. However, these areas were calculated in two dimensions (flat), which underestimates the true extent of *M. oculata* habitats located on the canyon flanks. If three-dimensional models were used, as demonstrated in prior photogrammetry studies (Fabri *et al.*, 2019; Fabri *et al.*, 2022), it is likely that the values for *M. oculata* would be significantly higher. This discrepancy highlights a limitation of 2-D mapping, particularly for habitats situated on steep or vertical canyon walls. Interestingly, previous studies comparing colony numbers rather than surface area reported up to 10 times (Gori *et al.*, 2013) or 2.2 times (Fabri *et al.*, 2022) more *M. oculata* colonies than *D. pertusum*. However, in high density areas, colonies in thickets (bushes) are difficult to distinguish from each other, particularly as some of them can form chimaera colonies (Arnaud-Haond *et al.*, 2017; Lartaud *et al.*, 2019) and the quality of images and videos also plays a significant role in the accuracy of colony counts. Yet, when comparing habitat surface areas, *D. pertusum* dominates at the canyon scale.

ROV explorations in the Lacaze-Duthiers Canyon confirm a depth-related pattern, with *D. pertusum* occurring deeper than *M. oculata* (Gori *et al.*, 2013; Fabri *et al.*, 2022). This pattern aligns with habitat preference studies focused on growth rates and microbiology (Lartaud *et al.*, 2017; Chapron *et al.*, 2020a). In the deepest areas, *D. pertusum* is found preferentially on gentler slopes at the base of canyon walls, where outcrops of boulders emerge from eroded sediments or have been detached from overlying walls.

Models and *in situ* observations confirm overlapping habitats (Fabri *et al.*, 2022), particularly along the western flank in rugged niches, and at the spurs formed between the tributaries of the canyon flank and the main canyon axis. These topographic features create outgrowths along the canyon flanks (Fig. 10 in Fabri *et al.*, 2022). Flows coming from both directions - along the main canyon and from the tributaries near the canyon head - can converge at these points, creating hydrodynamic conditions that favor *D. pertusum* growth, especially on the western flank, where the largest colonies have been observed (Fabri *et al.*, 2022). At these sites, *D. pertusum* colonies can reach up to 90 cm in height, forming clumps up to 2.5 meters long, while *M. oculata* colonies grow up to 50 cm high and 1.8 meters in length (Fabri *et al.*, 2022).

Fishing pressure

The SAR abrasion index derived from VMS data, indicated an absence of fishing pressure from trawling within the Lacaze-Duthiers Canyon head itself, and relatively low pressure around the canyon head. The AFE provided by GFW using AIS data, which resolves fishing effort at a higher resolution, suggests a certain level of fishing pressure to the west and east of the Lacaze-Duthiers Canyon head. These areas coincide with the distribution limit of CWC along the canyon's western and eastern flanks, highlighting potential threats to these species.

The SAR abrasion index is calculated based on 1' x 1' resolution cells, which averages the pressure data over the entire cell. Consequently, highly localized and intense pressure may appear negligible when averaged over the cell area. Furthermore, VMS positioning data is recorded every two hours for Spanish vessels and every hour for French vessels, which may be insufficient to accurately capture short-duration fishing activities. In contrast, AIS data is collected every minute and provides a better representation of fishing vessel presence. Since VMS data are used to monitor fishing vessel activities as part of fisheries regulation and management, we recommend increasing the VMS positioning transmission frequency across all European countries and developing robust tools to monitor and assess fishing pressure and its resulting footprint on the seabed by integrating both VMS and AIS data systems.

Longline fishing, which is not accounted for in the SAR abrasion index calculation, is included in the AFE. However, no longliners were recorded in the two extraction polygons we drew on the shelf. However, abandoned longlines are the most frequently observed fishing gear entangled in CWC. Long-abandoned longlines are often colonized by oysters or even corals, whereas newer ones are much less visible as they have not yet been covered by epifauna. I*n situ* observations confirm that the most direct observable impact on corals is primarily caused by longliners. This is particularly true on the flanks of the canyon when longlines fall into the canyon unintentionally. Lost fishing gear in western Mediterranean canyons has been reported at an average of approximately three

items/km (Fabri *et al.*, 2014; Tubau *et al.*, 2015). When considering surface areas, an overall density of 16 cm/m² was found on the canyon flanks, reaching up to 30 cm / m² in some locations (Fabri *et al.*, 2022). The most severe damage occurs when fishermen attempt to retrieve entangled lines, often inadvertently causing significant harm to corals (Ragnarsson *et al.*, 2017). Derelict fishing lines impact animal forests living in Mediterranean canyons, as documented in Ligurian canyons (Cau *et al.*, 2017; Consoli *et al.*, 2019; Giusti *et al.*, 2019; Angiolillo *et al.*, 2021; Bo *et al.*, 2023) and western Mediterranean canyons (Fabri *et al.*, 2014; Tubau *et al.*, 2015; Lastras *et al.*, 2016; Bilan *et al.*, 2025). In addition to fishing lines, trawl nets can also end up in the canyon, likely due to 'accidents' when trawlers navigate too close to the canyon rim or when strong currents carry the gear away from the intended fishing ground. The net can then become entangled in rocky outcrops or corals (Fig. 10).

Trawling on the continental shelf around canyon heads can also cause continuous sediment resuspension, indirectly impacting the animal forests below (Bilan *et al.*, 2023). Once in suspension, these sediments can be transported by currents and eventually settle into the underlying canyon, leading to increased sedimentation rates (Martin *et al.*, 2008; Puig *et al.*, 2015; Paradis *et al.*, 2017; Paradis *et al.*, 2018). At the rim of the Lacaze-Duthiers Canyon, bottom currents simulated in the SYMPHONIE hydrodynamic model showed that currents originating from the western and eastern shelves flow downward toward the canyon axis (Appendix D), carrying resuspended material into its depths. This anthropogenic sediment input could pose a threat to sessile species living in the Lacaze-Duthiers Canyon, including corals, as they face the risk of burial and suffocation (Chapron *et al.*, 2020b; Bilan *et al.*, 2023). However, the dense shelf water cascades observed in this canyon play a crucial role in resuspending and transporting these sediments further down-canyon (Canals *et al.*, 2006; Palanques *et al.*, 2006a; Ogston *et al.*, 2008; Canals *et al.*, 2009; Durrieu de Madron *et al.*, 2023), regularly "cleansing" fixed benthic species, a process essential to maintain coral colony growth (Chapron *et al.*, 2020b). To date, this natural mechanism has appeared to mitigate the negative effects of excessive sedimentation due to bottom trawling resuspension on corals and other benthic organisms.

Nevertheless, climate change in the Mediterranean, including the warming of surface (0-100 m) and intermediate (200-600 m) waters in the Mediterranean over the 21st century (Reale *et al.*, 2022), is expected to lead to a decline in cascading phenomena (Herrmann *et al.*, 2008; Durrieu de Madron *et al.*, 2023), thereby increasing the risks faced by deep-sea ecosystems. Such a reduction in intensity and recurrence of dense shelf water formation has already been observed in the Lacaze-Duthiers Canyon over the last 10 years (Durrieu de Madron *et al.*, 2023). These threats, combined with deep-sea temperature increase, ocean acidification and a decrease in aragonite saturation (Hennige *et al.*, 2020; Chemel *et al.*, 2024), are likely to weaken coral habitats and reduce biodiversity, highlighting the urgent need for effective conservation strategies.

The Natura 2000 site "Récifs des canyons Lacaze-Duthiers, Pruvot et Bourcart" (https://inpn.mnhn.fr/site/natura2000/FR9102016) has been identified by the French government as a candidate for a strong protection zone by 2027, following the public debate "*la mer en débat" (https://www.mer.gouv.fr/la-mer-en-debat)*, which included discussions on mapping priority marine and terrestrial areas for offshore wind power (Ministère du partenariat avec les territoires et de la décentralisation, 2024). In this context, our study provides key insights for decision-makers and managers in designing and implementing protection measures, including addressing indirect impacts such as sediment fallout from the overlying continental shelf, located outside the canyon boundaries. These findings further support the extention of the N2000 site to safeguard the colonial scleractinians on the Lacaze-Duthiers canyon's flanks. The AFE data reveal a recurrently visited fishing ground along the western and eastern edges of the canyon. This fishing activity, due to its proximity to living corals downslope, exerts pressure on these vulnerable organisms, which are negatively impacted by lost fishing gear and increased sediment deposition. Consequently, it is evident that the establishment of a reinforced protection zone should not be limited to the Lacaze-Duthiers Canyon itself but should also extend to the surrounding shelf around the canyon head – particularly where both bottom trawling pressure and the concentration of living corals are the highest.

Given the cross-border nature of the Lacaze-Duthiers Canyon, any protection initiatives must involve collaboration with Spain, as French regulations alone do not apply to Spanish fishermen. Finally, it is critical to develop fisheries management measures tailored to the sensitivity of colonial scleractinian habitats, with the active involvement of fishermen and other stakeholders in a concerted effort. Such targeted actions will enable the preservation of CWC while ensuring the sustainable management of fishing activities.

Acknowledgements

This research was funded, in part, by the REDRESS European project (Restoration of Deep-Sea Habitats to Rebuild European Seas https://redress-project.eu/) No 101135492. The hydrodynamic simulations were performed with support from the national SIROCCO service (ILICO research infrastructure) using HPC resources from CALMIP (grant P09115). We gratefully acknowledge grant CEX2024-001494-S to ICM-CSIC funded by AEI 10.13039/501100011033. We are also grateful to all the participants of the CALADU_2019 cruise (doi:10.17600/18000929), CALADU_2021 cruise (doi: 10.17600/18001575); IMPEC_2021 cruise (doi: 10.17600/18001594); PLAS-SCORE_2023 cruise (doi: 10.17600/18002068); ECALION cruise in 2023 especially S. Hourdez (P.I. with N. Michez) and Medseacan cruise (P.I. P. Watremez) in 2009. We also thank C. Labrune for her reading. Furthermore, we are indebted to Keith Hod-

son for correcting the English. The authors also thank the reviewers for their helpful comments aimed at improving the manuscript. A CC-BY public copyright license has been applied by the authors to the present document and will be applied to all subsequent versions up to the Author Accepted Manuscript arising from this submission, in accordance with the grant's open access conditions.

References

Amoroso, R.O., Pitcher, C.R., Rijnsdorp, A.D., McConnaughey, R.A., Parma, A.M. *et al.*, 2018. Bottom trawl fishing footprints on the world's continental shelves, *Proceedings of the National Academy of Sciences of the United States of America*. 115 (43), E10275-E10282.

Angiolillo, M., Gérigny, O., Valente, T., Fabri, M.-C., Tambute, E. *et al.*, 2021. Distribution of seafloor litter and its interaction with benthic organisms in deep waters of the Ligurian Sea (Northwestern Mediterranean). *Science of the Total Environment*, 788, 147745.

Arnaud-Haond, S., Van den Beld, I.M.J., Becheler, R., Orejas, C., Menot, L. *et al.*, 2017. Two "pillars" of cold-water coral reefs along Atlantic European margins: Prevalent association of *Madrepora oculata* with *Lophelia pertusa*, from reef to colony scale. *Deep Sea Research Part II: Topical Studies in Oceanography*, 145, 110-119.

Baldwin, R.A., 2009. Use of Maximum Entropy Modeling in Wildlife Research, *Entropy*, 11 (4), 854-866.

Bargain, A., Foglini, F., Pairaud, I., Bonaldo, D., Carniel, S. *et al.*, 2018. Predictive habitat modeling in two Mediterranean canyons including hydrodynamic variables. *Progress in Oceanography*, 169, 151-168.

Bilan, M., Gori, A., Grinyó, J., Biel-Cabanelas, M., Puigcerver-Segarra, X. *et al.*, 2023. Vulnerability of six cold-water corals to sediment resuspension from bottom trawling fishing. *Marine Pollution Bulletin*, 196, 115423.

Bilan, M., Grinyó, J., Cabrera, C., Gori, A., Santín, A. *et al.*, 2025. The hanging gardens of Blanes Canyon, Northwestern Mediterranean Sea. *Deep Sea Research Part I: Oceanographic Research Papers*, 221, 104514.

Bo, M., Enrichetti, F., Betti, F., Gay, G., Quarta, G. *et al.*, 2023. The cold-water coral province of the eastern Ligurian Sea (NW Mediterranean Sea): historical and novel evidences. *Frontiers in Marine Science*, 10, 1114417.

Bramanti, L., Maria Carla, Benedetti, R., Cupido, O., Cocito, S. *et al.*, 2017. Demography of Animal Forests: The Example of Mediterranean Gorgonians. p. 548-567. In: *Marine Animal Forest*. Rossi, S., Bramanti, L., Gori, A., Orejas, C. (Eds.). Springer International Publishing, Cham, Switzerland.

Brooke, S., Ross, S.W., Bane, J.M., Seim, H.E., Young, C.M., 2013. Temperature tolerance of the deep-sea coral *Lophelia pertusa* from the southeastern United States. *Deep-Sea Research Part Ii-Topical Studies in Oceanography*, 92, 240-248.

Canals, M., Danovaro, R., Marco Luna, G., 2019. Recent advances in understanding the ecology and functioning of submarine canyons in the Mediterranean Sea. *Progress in Oceanography*, 179, 102171.

Canals, M., Puig, P., Durrieu de Madron, X., Heussner, S., Palanques, A. *et al.*, 2006. Flushing submarine canyons. *Nature*, 444 (7117), 354-357.

Canals, M., Danovaro, R., Heussner, S., Lykousis, V., Puig, P. *et al.*, 2009. Cascades in mediterranean submarine grand canyons. *Oceanography*, 22 (1), 26-43.

Cau, A., Alvito, A., Moccia, D., Canese, S., Pusceddu, A. *et al.*, 2017. Submarine canyons along the upper Sardinian slope (Central Western Mediterranean) as repositories for derelict fishing gears. *Marine Pollution Bulletin*, 123 (1), 357-364.

Chapron, L., Lartaud, F., Le Bris, N., Peru, E., Galand, P.E., 2020a. Local Variability in Microbiome Composition and Growth Suggests Habitat Preferences for Two Reef-Building Cold-Water Coral Species. *Frontiers in Microbiology*, 11 (275).

Chapron, L., Le Bris, N., Durrieu de Madron, X., Peru, E., Galand, P.E. *et al.*, 2020b. Long term monitoring of cold-water coral growth shows response to episodic meteorological events in the NW Mediterranean. *Deep Sea Research Part I: Oceanographic Research Papers*, 160, 103255.

Chapron, L., Galand, P.E., Pruski, A.M., Peru, E., Vetion, G. *et al.*, 2021. *Resilience of cold-water coral holobionts to thermal stress. Proceedings of the Royal Society B-Biological Sciences*, 288 (1965), 20212117.

Chemel, M., Peru, E., Binsarhan, M., Logares, R., Lartaud, F. *et al.*, 2024. Cold-water coral mortality under ocean warming is associated with pathogenic bacteria. *Environmental Microbiome*, 19 (1), 76.

Consoli, P., Romeo, T., Angiolillo, M., Canese, S., Esposito, V. *et al.*, 2019. Marine litter from fishery activities in the Western Mediterranean sea: The impact of entanglement on marine animal forests. *Environmental Pollution*, 249, 472-481.

Davies, A.J., Wisshak, M., Orr, J.C., Roberts, J.M., 2008. Predicting suitable habitat for the cold-water coral *Lophelia pertusa* (Scleractinia). *Deep-Sea Research Part I-Oceanographic Research Papers*, 55 (8), 1048-1062.

Davies, A.J., Guinotte, J.M., 2011. Global Habitat Suitability for Framework-Forming Cold-Water Corals. *Plos One*, 6 (4), e18483.

Davies, J.S., Guillaumont, B., Tempera, F., Vertino, A., Beuck, L. *et al.*, 2017. A new classification scheme of European cold-water coral habitats: Implications for ecosystem-based management of the deep sea. *Deep Sea Research Part II: Topical Studies in Oceanography*, 145, 102-109.

Durrieu de Madron, X., Ferre, B., Le Corre, G., Grenz, C., Conan, P. *et al.*, 2005. Trawling-induced resuspension and dispersal of muddy sediments and dissolved elements in the Gulf of Lion (NW Mediterranean). *Continental Shelf Research*, 25, 2387-2409.

Durrieu de Madron, X., Houpert, L., Puig, P., Sanchez-Vidal, A., Testor, P. *et al.*, 2013. Interaction of dense shelf water cascading and open-sea convection in the northwestern Mediterranean during winter 2012. *Geophysical Research Letters*, 40 (7), 1379-1385.

Durrieu de Madron, X., Aubert, D., Charrière, B., Kunesch, S., Menniti, C. *et al.*, 2023. Impact of Dense Water Formation on the Transfer of Particles and Trace Metals from the Coast to the Deep in the Northwestern Mediterranean. *Water*, 15 (301).

Eigaard, O.R., Bastardie, F., Hintzen, N.T., Buhl-Mortensen,

L., Buhl-Mortensen, P. *et al.*, 2017. The footprint of bottom trawling in European waters: distribution, intensity, and seabed integrity. *Ices Journal of Marine Science*, 74 (3), 847-865.

Elith, J., Phillips, S.J., Hastie, T., Dudík, M., Chee, Y.E. *et al.*, 2011. A statistical explanation of MaxEnt for ecologists. *Diversity and Distributions*, 17 (1), 43-57.

Estournel, C., Fabri, M.-C., 2025. *Near-seafloor hydrodynamic data in the western Gulf of Lion, 1 Nov 2012-15 April 2014*. Ifremer SEANOE.

Estournel, C., Marsaleix, P., Ulses, C., 2021. A new assessment of the circulation of Atlantic and Intermediate Waters in the Eastern Mediterranean. *Progress in Oceanography*, 198, 102673.

Estournel, C., Mikolajczak, G., Ulses, C., Bourrin, F., Canals, M. *et al.*, 2023. Sediment dynamics in the Gulf of Lion (NW Mediterranean Sea) during two autumn–winter periods with contrasting meteorological conditions. *Progress in Oceanography*, 210, 102942.

EU, 1992. Directive 92/43/EEC of the Council of the 21 May 1992 on the conservation of natural habitats and of wild fauna and flora. *Official Journal of the European Communities* L206, 1-44.

EU, 2008a. Regulation 734/2008/EC of the 15 July 2008 on the protection of vulnerable marine ecosystems in the high seas from the adverse impacts of bottom fishing gears. *Official Journal of the European Communities* L201, 1-6.

EU, 2008b. Directives 2008/56/EC of the European Parliament and of the Council of 17 June 2008 establishing a framework for community action in the field of marine environmental policy (Marine Strategy Framework Directive). *Official Journal of the European Communities* L164, 1-22.

EU, 2017. Directive 2017/845/EU of the 17 May 2017 amending Directive 2008/56/EC of the European Parliament and of the Council as regards the indicative lists of elements to be taken into account for the preparation of marine strategies. *Official Journal of the European Communities* L125, 27-33.

EU, 2023. Regulation P9_TA(2023)0277 of the European Parliament and of the Council of 12 July 2023 on nature restoration. *Official Journal of the European Communities* Document A9-0220/2023, 1-153.

Fabri, M.C., Pedel, L., Beuck, L., Galgani, F., Hebbeln, D. *et al.*, 2014. Megafauna of vulnerable marine ecosystems in French mediterranean submarine canyons: Spatial distribution and anthropogenic impacts. *Deep-Sea Research Part Ii-Topical Studies in Oceanography*, 104, 184-207.

Fabri, M.C., Bargain, A., Pairaud, I., Pedel, L., Taupier-Letage, I., 2017. Cold-water coral ecosystems in Cassidaigne Canyon: An assessment of their environmental living conditions. *Deep Sea Research Part II: Topical Studies in Oceanography*, 137, 436-453.

Fabri, M.-C., Vinha, B., Allais, A.-G., Bouhier, M.-E., Dugornay, O. *et al.*, 2019. Evaluating the ecological status of cold-water coral habitats using non-invasive methods: An example from Cassidaigne canyon, northwestern Mediterranean Sea. *Progress in Oceanography*, 178, 102172.

Fabri, M.-C., Dugornay, O., de la Bernardie, X., Guerin, C., Sanchez, P. *et al.*, 2022. 3D-Representations for studying deep-sea coral habitats in the Lacaze-Duthiers Canyon, from geological settings to individual specimens. *Deep Sea Research Part I: Oceanographic Research Papers*, 187, 103831.

Fabri, M.-C., Dreidemy, J., 2024a. *Bathymetry and seafloor variables at 5-m resolution in the Lacaze-Duthiers Canyon, below130 m depth*. Ifremer Sextant. https://doi.org/10.12770/1cc30b12-ad4e-415f-8f1f-ad690e0c266c

Fabri, M.-C., Dreidemy, J., 2024b. *Bathymetry and seafloor variables at 10-m resolution in the Lacaze-Duthiers Canyon, below130 m depth*. Ifremer Sextant. https://doi.org/10.12770/45218382-4036-4c14-b09c-c3bef3484e80

Fabri, M.-C., Estournel, C., 2024a. *Hydrodynamic variables at 10-m resolution in the Lacaze-Duthiers Canyon, below130 m depth*. Ifremer Sextant. https://doi.org/10.12770/a6e2a978-7f85-4054-ab63-c71478a228cb

Fabri, M.-C., Estournel, C., 2024b. *Hydrodynamic variables at 5-m resolution in the Lacaze-Duthiers Canyon, below130 m depth*. Ifremer Sextant. https://doi.org/10.12770/f425108e-1b7d-4a3c-aae2-7942d42b56ca

Fabri, M.-C., Dreidemy, J., Lartaud, F., Michez, N., 2025a. *Presence and absence of cold-water coral in the Lacaze-Duthiers Canyon, at a 10-m resolution*. Ifremer Sextant. https://doi.org/10.12770/2c683158-d02b-460f-a60a-e748c593279f

Fabri, M.-C., Dreidemy, J., Lartaud, F., Michez, N., 2025b. *Probable habitats of two cold-water coral species (suitability > 70%), in the Lacaze-Duthiers Canyon*. Ifremer Sextant. https://doi.org/10.12770/36301f2c-0a2b-4c64-bd81-aaa370366d4a

Fabri, M.-C., Dreidemy, J., Lartaud, F., Michez, N., 2025c. *Presence and absence of Desmophyllum pertusum (syn. Lophelia pertusa) in the Lacaze-Duthiers Canyon, at a 5-m resolution*. Ifremer Sextant. https://doi.org/10.12770/0c56f019-5360-4676-b542-61b1e478b0d3

Fabri, M.-C., Dreidemy, J., Lartaud, F., Michez, N., 2025d. *Presence and absence of Madrepora oculata in the Lacaze-Duthiers Canyon, at a 5-m resolution*. Ifremer Sextant. https://doi.org/10.12770/1edf0153-b1d9-489f-9401-3592d5a3535f

Fabri, M.-C., Lartaud, F., Michez, N., 2025e. *Cold-Water Coral observation points in the Lacaze-Duthiers canyon, 2008-2023*. Ifremer SEANOE. https://doi.org/10.17882/105454

FAO, 2016. *Vulnerable Marine Ecosystems : Processes and Practices in the High Seas*. FAO Fisheries and Aquaculture Technical Paper No. 595pp.

Fiala-Medioni, A., Madurell, T., Romans, P., Reyss, D., Pibot, A. *et al.*, 2012. ROV and submersible surveys on faunal assemblages in a deep-sea canyon (Rech Lacaze-Duthiers, Western Mediterranean Sea). *Vie Et Milieu-Life and Environment*, 62 (4), 173-190.

Fink, H.G., Wienberg, C., De Pot-Holz, R., Hebbeln, D., 2015. Spatio-temporal distribution patterns of Mediterranean cold-water corals (Lophelia pertusa and Madrepora oculata) during the past 14,000 years. *Deep-Sea Research Part I-Oceanographic Research Papers*, 103, 37-48.

Freiwald, A., Beuck, L., Rüggeberg, A., Taviani, M., Hebbeln, D., 2009. The white coral community in the Central Mediterranean Sea revealed by ROV Surveys. *Oceanography*, 22 (1), 58-74.

Georges, V., Begot, E., Duchene, J., Fabri, M.C., Laffargue, P.

et al., 2021. *Développement d'un indicateur d'abrasion des fonds marins par les arts de pêche trainants pour l'évaluation du bon état écologique des habitats benthiques*. Ifremer Technical report, No LEP 21-04, 19 pp.

GFCM, 2009. *Criteria for the identification of sensitive habitats of relevance for the management of priority species*. Scientific Advisory Committee (SAC) - Sub-Committee on Marine Environment and Ecosystems (SCMEE), General Fisheries Commission for the Mediterranean, 3 pp.

GFCM, 2018. *Report of the second meeting of the Working Groups on Vulnerable Marine Ecosystems (WGVME), 28 Feb. 2018*. Working Group on Vulnerable Marine Ecosystems (WGVME), FAO, 57 pp.

GFCM, 2019. *Third Report of the Working group on Marine Protected Areas (WGMPA), including a session on essential fish habitat (EFH), 18-21 Feb 2019*. Scientific Advisory Committee on Fisheries (SAC), FAO, 53 pp.

Giusti, M., Canese, S., Fourt, M., Bo, M., Innocenti, C. *et al.*, 2019. Coral forests and Derelict Fishing Gears in submarine canyon systems of the Ligurian Sea. *Progress in Oceanography*, 178, 102186.

Gori, A., Orejas, C., Madurell, T., Bramanti, L., Martins, M. *et al.*, 2013. Bathymetrical distribution and size structure of cold-water coral populations in the Cap de Creus and Lacaze-Duthiers canyons (northwestern Mediterranean). *Biogeosciences*, 10 (3), 2049-2060.

Guisan, A., Edwards Jr, T.C., Hastie, T., 2002. Generalized linear and generalized additive models in studies of species distributions: setting the scene. *Ecological Modelling*, 157 (2-3), 89-100.

Hennige, S.J., Wolfram, U., Wickes, L., Murray, F., Roberts, J.M. *et al.*, 2020. Crumbling Reefs and Cold-Water Coral Habitat Loss in a Future Ocean: Evidence of "Coralporosis" as an Indicator of Habitat Integrity. *Frontiers in Marine Science*, 7, 668.

Herrmann, M., Estournel, C., Déqué, M., Marsaleix, P., Sevault, F. *et al.*, 2008. Dense water formation in the Gulf of Lions shelf: Impact of atmospheric interannual variability and climate change. *Continental Shelf Research*, 28 (15), 2092-2112.

Ifremer, 2021. *ALGOPESCA geolocation data processing algorithm*. Ifremer RBE/STH/LBH Archimer ID 79405, 27 pp.

Ifremer, 2024. *Abrasion superficielle des fonds marins par les arts de pêche trainants*. Ifremer Sextant. https://doi.org/10.12770/ec189ce9-05bd-4580-b5f3-4851e9f31df0

Ifremer Geo-Ocean, 2023a. *Bathymétrie - golfe du Lion, canyon Lacaze-Duthiers, résolution 10 m (campagne CALADU_2021, 2021).* Ifremer Sextant. https://doi.org/10.12770/e4869a28-ba86-4348-a111-22aea0efa54f

Ifremer Geo-Ocean, 2023b. *Bathymétrie - golfe du Lion, canyon Lacaze-Duthiers, résolution 5 m (campagne CALADU_2021, 2021)*. Ifremer Sextant. https://doi.org/10.12770/74492729-a034-42ee-a517-7037cda010b4

Kroodsma, D.A., Mayorga, J., Hochberg, T., Miller, N.A., Boerder, K.*, et al.*, 2018. Tracking the global footprint of fisheries. *Science*, 359 (6378), 904-908.

Lacaze-Duthiers, H., 1897. *Archives de zoologie expérimentale et générale*. (S. Frères, Ed.) C. Reinwald, Paris, 532 p. pp.

Lartaud, F., Meistertzheim, A.L., Peru, E., Le Bris, N., 2017. In situ growth experiments of reef-building cold-water corals: The good, the bad and the ugly. *Deep-Sea Research Part I-Oceanographic Research Papers*, 121, 70-78.

Lartaud, F., Mouchi, V., Chapron, L., Meistertzheim, A.L., Le Bris, N., 2019. 36 Growth Patterns of Mediterranean Calcifying Cold-Water Corals. p. 405-422. In: *Mediterranean Cold-Water Corals: Past, Present and Future*. Orejas, C., Jiménez, C. (Eds.). Springer, Cham, Switzerland.

Lastras, G., Canals, M., Ballesteros, E., Gili, J.M., Sanchez-Vidal, A., 2016. Cold-Water Corals and Anthropogenic Impacts in La Fonera Submarine Canyon Head, Northwestern Mediterranean Sea. *PloS One*, 11 (5).

Lo Iacono, C., Robert, K., Gonzalez-Villanueva, R., Gori, A., Gili, J.-M. *et al.*, 2018. Predicting cold-water coral distribution in the Cap de Creus Canyon (NW Mediterranean): implications for marine conservation planning. *Progress in Oceanography*, 169, 169-180.

Lunden, J.J., McNicholl, C.G., Sears, C.R., Morrison, C.L., Cordes, E.E., 2014. Acute survivorship of the deep-sea coral *Lophelia pertusa* from the Gulf of Mexico under acidification, warming, and deoxygenation. *Frontiers in Marine Science*, 1, 1-12.

Many, G., Ulses, C., Estournel, C., Marsaleix, P., 2021. Particulate organic carbon dynamics in the Gulf of Lion shelf (NW Mediterranean) using a coupled hydrodynamic–biogeochemical model. *Biogeosciences*, 18, 5513-5538.

Marsaleix, P., Auclair, F., Estournel, C., 2006. Considerations on open boundary conditions for regional and coastal ocean models. *Journal of Atmospheric and Oceanic Technology*, 23 (11), 1604-1613.

Marsaleix, P., Ulses, C., Pairaud, I., Herrmann, M.J., Floor, J.W. *et al.*, 2009. Open boundary conditions for internal gravity wave modelling using polarization relations. *Ocean Modelling*, 29 (1), 27-42.

Martin, J., Puig, P., Palanques, A., Masque, P., Garcia-Orellana, J., 2008. Effect of commercial trawling on the deep sedimentation in a Mediterranean submarine canyon. *Marine Geology*, 252 (3-4), 150-155.

Matos, F.L., Ross, S.W., Huvenne, V.A.I., Davies, J.S., Cunha, M.R., 2018. Canyons pride and prejudice: Exploring the submarine canyon research landscape, a history of geographic and thematic bias. *Progress in Oceanography*, 169, 6-19.

Matos, F.L., Company, J.B., Cunha, M.R., 2021. Mediterranean seascape suitability for *Lophelia pertusa*: Living on the edge. *Deep-Sea Research Part I-Oceanographic Research Papers*, 170 (103496).

Mikolajczak, G., Estournel, C., Ulses, C., Marsaleix, P., Bourrin, F. *et al.*, 2020. Impact of storms on residence times and export of coastal waters during a mild autumn/winter period in the Gulf of Lion. *Continental Shelf Research*, 207 (104192).

Ministère du partenariat avec les territoires et de la décentralisation, 2024. Décision du 17 octobre 2024 consécutive au débat public « la mer en débat » portant sur la mise à jour des volets stratégiques des documents stratégiques de façade et la cartographie des zones maritimes et terrestres prioritaires pour l'éolien en mer. 38 pp.

Mohn, C., Rengstorf, A., White, M., Duineveld, G., Mienis, F. *et al.*, 2014. Linking benthic hydrodynamics and cold-water coral occurrences: A high-resolution model study at three

cold-water coral provinces in the NE Atlantic. *Progress in Oceanography*, 122, 92-104.

Ogston, A.S., Drexler, T.M., Puig, P., 2008. Sediment delivery, resuspension, and transport in two contrasting canyon environments in the southwest Gulf of Lions. *Continental Shelf Research*, 28 (15), 2000-2016.

Orejas, C., Gori, A., Rad-Menendez, C., Last, K.S., Davies, A.J. *et al.*, 2016. The effect of flow speed and food size on the capture efficiency and feeding behaviour of the cold-water coral Lophelia pertusa. *Journal of Experimental Marine Biology and Ecology*, 481, 34-40.

Palanques, A., Durrieu de Madron, X., Puig, P., Fabres, J., Guillen, J. *et al.*, 2006a. Suspended sediment fluxes and transport processes in the Gulf of Lions submarine canyons. The role of storms and dense water cascading. *Marine Geology*, 234 (1-4), 43-61.

Palanques, A., Martin, J., Puig, P., Guillen, J., Company, J.B. *et al.*, 2006b. Evidence of sediment gravity flows induced by trawling in the Palamos (Fonera) submarine canyon (northwestern Mediterranean). *Deep-Sea Research Part I-Oceanographic Research Papers*, 53 (2), 201-214.

Palanques, A., Puig, P., Latasa, M., Scharek, R., 2009. Deep sediment transport induced by storms and dense shelf-water cascading in the northwestern Mediterranean basin. *Deep-Sea Research Part I-Oceanographic Research Papers*, 56, 425-434.

Palanques, A., Puig, P., de Madron, X.D., Sanchez-Vidal, A., Pasqual, C. *et al.*, 2012. Sediment transport to the deep canyons and open-slope of the western Gulf of Lions during the 2006 intense cascading and open-sea convection period. *Progress in Oceanography*, 106, 1-15.

Paradis, S., Puig, P., Masqué, P., Juan-Díaz, X., Martín, J. *et al.*, 2017. Bottom-trawling along submarine canyons impacts deep sedimentary regimes. *Scientific Reports*, 7 (1), 43332.

Paradis, S., Puig, P., Sanchez-Vidal, A., Masque, P., Garcia-Orellana, J. *et al.*, 2018. Spatial distribution of sedimentation-rate increases in Blanes Canyon caused by technification of bottom trawling fleet. *Progress in Oceanography*, 169, 241-252.

Pasqual, C., Sanchez-Vidal, A., Zuniga, D., Calafat, A., Canals, M. *et al.*, 2010. Flux and composition of settling particles across the continental margin of the Gulf of Lion: the role of dense shelf water cascading. *Biogeosciences*, 7 (1), 217-231.

Pearman, T.R.R., Robert, K., Callaway, A., Hall, R., Lo Iacono, C. *et al.*, 2020. Improving the predictive capability of benthic species distribution models by incorporating oceanographic data - Towards holistic ecological modelling of a submarine canyon. *Progress in Oceanography*, 184, 102338.

Peres, J.M., Picard, J., 1964. *Nouveau Manuel de Bionomie benthique de la mer Méditerranée*. Station Marine d'Endoûme, Marseille, 137 pp.

Petrenko, A.A., Doglioli, A.M., Nencioli, F., Kersalé, M., Hu, Z.Y. *et al.*, 2017. A review of the LATEX project: mesoscale to submesoscale processes in a coastal environment. *Ocean Dynamics*, 67, 513-533.

Phillips, S.J., Anderson, R.P., Schapire, R.E., 2006. Maximum entropy modeling of species geographic distributions. *Ecological Modelling*, 190, 231-259.

Phillips, S.J., Dudik, M., Schapire, R.E., 2019. *Maxent software for modeling species niches and distributions (V 3.4.1; Accessed 18 June 2019)*. http://biodiversityinformatics.amnh.org/open_source/maxent/

Poncelet, C., Billant, G., Corre, M.-P., 2020. *Globe (Global Oceanographic Bathymetry Explorer) Software. (V1.17.10; Accessed 10 August 2021)*. Ifremer. https://doi.org/10.17882/70460

Puig, P., Palanques, A., Orange, D.L., Lastras, G., Canals, M., 2008. Dense shelf water cascades and sedimentary furrow formation in the Cap de Creus Canyon, northwestern Mediterranean Sea. *Continental Shelf Research*, 28 (15), 2017-2030.

Puig, P., Canals, M., Company, J.B., Martin, J., Amblas, D. *et al.*, 2012. Ploughing the deep sea floor. *Nature*, 489 (7415), 286-289.

Puig, P., Martín, J., Masqué, P., Palanques, A., 2015. Increasing sediment accumulation rates in La Fonera (Palamós) submarine canyon axis and their relationship with bottom trawling activities. *Geophysical Research Letters*, 42 (19), 8106-8113.

Puig, P., Gili, J.-M., 2019. 27 Submarine Canyons in the Mediterranean: A Shelter for Cold-Water Corals. p. 285-289. In: *Mediterranean Cold-Water Corals: Past, Present and Future: Understanding the Deep-Sea Realms of Coral*. Orejas, C., Jiménez, C. (Eds.). Springer International Publishing, Cham.

Pusceddu, A., Bianchelli, S., Martin, J., Puig, P., Palanques, A. *et al.*, 2014. Chronic and intensive bottom trawling impairs deep-sea biodiversity and ecosystem functioning. *Proceedings of the National Academy of Sciences of the United States of America*, 111 (24), 8861-8866.

Ragnarsson, S.Á., Burgos, J.M., Kutti, T., van den Beld, I., Egilsdóttir, H. *et al.*, 2017. The Impact of Anthropogenic Activity on Cold-Water Corals. p. 989-1023. In: *Marine Animal Forests: The Ecology of Benthic Biodiversity Hotspots*. Rossi, S., Bramanti, L., Gori, A., Orejas, C. (Eds.). Springer International Publishing, Cham.

Reale, M., Cossarini, G., Lazzari, P., Lovato, T., Bolzon, G. *et al.*, 2022. Acidification, deoxygenation, and nutrient and biomass declines in a warming Mediterranean Sea. *Biogeosciences*, 19 (17), 4035-4065.

Rengstorf, A.M., Mohn, C., Brown, C., Wisz, M.S., Grehan, A.J., 2014. Predicting the distribution of deep-sea vulnerable marine ecosystems using high-resolution data: Considerations and novel approaches. *Deep-Sea Research Part I-Oceanographic Research Papers*, 93, 72-82.

Reyss, D., 1964. Contribution à l'étude du rech Lacaze-Duthiers, vallée sous-marine des côtes du Roussillon. *Vie et Milieu*, 15 (1), 1-46.

Sanchez-Vidal, A., Pasqual, C., Kerherve, P., Heussner, S., Calafat, A. *et al.*, 2009. Across margin export of organic matter by cascading events traced by stable isotopes, northwestern Mediterranean Sea. *Limnology and Oceanography*, 54 (5), 1488-1500.

Thuiller, W., Lafourcade, B., Engler, R., Araújo, M.B., 2009. BIOMOD - a platform for ensemble forecasting of species distributions (Version4.2-4). *Ecography*, 32 (3), 369-373.

Tong, R.J., Davies, A.J., Yesson, C., Yu, J.S.D., Luo, Y. *et al.*, 2023. Environmental drivers and the distribution of cold-water corals in the global ocean. *Frontiers in Marine*

Science, 10, 1217851.

Tubau, X., Canals, M., Lastras, G., Rayo, X., Rivera, J. *et al.*, 2015. Marine litter on the floor of deep submarine canyons of the Northwestern Mediterranean Sea: The role of hydrodynamic processes. *Progress in Oceanography*, 134, 379-403.

Ulses, C., Estournel, C., Bonnin, J., de Madron, X.D., Marsaleix, P., 2008a. Impact of storms and dense water cascading on shelf-slope exchanges in the Gulf of Lion (NW Mediterranean). *Journal of Geophysical Research-Oceans*, 113, C02010.

Ulses, C., Estournel, C., Puig, P., de Madron, X.D., Marsaleix, P., 2008b. Dense shelf water cascading in the northwestern Mediterranean during the cold winter 2005: Quantification of the export through the Gulf of Lion and the Catalan margin. *Geophysical Research Letters*, 35 (7).

Vertino, A., Savini, A., Rosso, A., Di Geronimo, I., Mastrototaro, F. *et al.*, 2010. Benthic habitat characterization and distribution from two representative sites of the deep-water SML Coral Province (Mediterranean). *Deep Sea Research Part II: Topical Studies in Oceanography*, 57 (5-6), 380-396.

Vierod, A.D.T., Guinotte, J.M., Davies, A.J., 2014. Predicting the distribution of vulnerable marine ecosystems in the deep sea using presence-background models. *Deep Sea Research Part II: Topical Studies in Oceanography*, 99, 6-18.

Watremez, P., 2012. Canyon heads in the French Mediterranean Sea - Overview of results from the MEDSEACAN and CORSEACAN campaigns (2008-2010). p. 105-112. In: *Mediterranean Submarine Canyons: Ecology and Governance*. Wurtz, M. (Ed.). IUCN, Gland, Switzerland.

Wilson, M.F.J., O'Connell, B., Brown, C., Guinan, J.C., Grehan, A.J., 2007. Multiscale Terrain Analysis of Multibeam Bathymetry Data for Habitat Mapping on the Continental Slope. *Marine Geodesy*, 30 (1-2), 3-35.

Zibrowius, H., 2003. *La communauté des "coraux blancs", les faunes des canyons et des montagnes sous-marines de la Mediterranée profonde*. Plan d'Action Stratégique pour la Conservation de la Biodiversité dans la Région Méditerranéenne (PAS BIO), 43 pp.

Supplementary Data

The following supplementary information is available online for the article:

Table S1. Summary of ROV dives used to extract coral observation points.

Appendix A. Selection of uncorrelated variables.

Appendix B. Response curves and validations obtained with GAM.

Appendix C. Model validation with Maxent.

Appendix D. Current flows around and in the Lacaze-Duthiers canyon.

Table S2. Apparent Fishing Effort extracted form Global Fishing Watch in the two selected polygon, gathering data from 2020 to 2023.